Supporting information

Aggregation polymorphism of photoactivatable Pt(IV) prodrugs as a strategy for the design of theranostic nanomaterials

Vladislav Bykusov[a]‡, Ilia Kuzmichev[a,b]‡, Maxim Stepanov[c], Dmitry Bunin[d], Yuriy Luponosov[e], Yulia Isaeva[a,e], Askold Trul[e], Roman Akasov[c], Alexander Erofeev[f], Regina Kuanaeva[a,f], Yulia Maksimova[g], Maxim Abakumov[b,f], Aleksey Nikitin[f], Vladimir Kuzmin[h], Anton Egorov[h], Ivan Burtsev[h], Igor A. Rodin[a], Mikhail F. Vokuev[a], Elena Beloglazkina[a], Olga Krasnovskaya[a]*‡

[a] Lomonosov Moscow State University, Chemistry Department, Leninskie Gory 1-3, Moscow, 119991, Russia;

[b] Department of Medical Nanobiotechnology, N.I. Pirogov Russian National Research Medical University, Ostrovityanova str., 1, 6, Moscow, 117997, Russia;

[c] Moscow Pedagogical State University (MPGU) 29/7 Malaya Pirogovskaya Str., building 1, Moscow, 119991, Russia;

[d] Frumkin Institute of Physical Chemistry and Electrochemistry Russian Academy of Sciences, 31-4, Leninsky prospect, 119071 Moscow, Russia;

[e] Enikolopov Institute of Synthetic Polymer Materials RAS, Profsoyuznaya st. 70, Moscow, 117393, Russia;

[f] National University of Science and Technology (MISIS), Leninskiy prospect 4, Moscow, 119049, Russia;

[g] Geological Institute of the Russian Academy of Sciences, Pyzhevsky per., 7, building 1, Moscow, 119017, Russia;

[h] Emanuel Institute of Biochemical Physics of the Russian Academy of Sciences, 119334, Kosygina str., b.4, Moscow, Russi

Table of contents.

1. Materials and methods

Acetic acid, 2-azidoacetic acid, boron trifluoride etherate ($BF_3 \cdot Et_2O$), cisplatin, 2,3-dichloride- 5,6-dicyano-p-benzoquinone (DDQ), 2,4-dimethyl-1*H*-pyrrole, N,N'-dicyclohexylcarbodiimide (DCC), hydrogen peroxide (30% w/w in water), 4-hydroxybenzaldehyde, propargyl bromide, potassium carbonate (K_2CO_3), sodium azide (NaN_3), sodium ascorbate, trifluoroacetic acid (TFA), triethylamine(Et_3N), 4-Nitrobenzaldehyde, pentafluorobenzaldehyde were used without purification. Acetone, acetonitrile (CH_3CN), dichloromethane (DCM, CH_2Cl_2), diethyl ether (Et_2O), methanol (MeOH), dimethylformamide (DMF), acetone, Pluronic® F127 (F127), DSPE-PEG_{2000}-OMe, dimethyl sulfoxide (DMSO) and petroleum ether were purchased from commercial sources and purified following the described procedures.[1]

Analytical thin-layer chromatography (TLC) was performed on Merck silica gel aluminum plates with F-254 indicator. Compounds were visualized by irradiation with UV light (254, 365 nm).

Preparative column chromatography was performed using Acros brand silica gel (60–200 mesh).

The NMR spectra were recorded on a Bruker Avance 400 MHz spectrometer (USA) in DMSO-d_6 and $CDCl_3$ with TMS as an internal standard for ^1H and ^{13}C and K_2PtCl_6 for ^{195}Pt NMR. All ^{13}C spectra were ^1H decoupled.

High-resolution mass spectra (HRMS) were recorded with a G3 QTof quadrupole-time-of-flight (Waters, USA) equipped with an ESI (ionization: ESI, capillary temperature 300 °C, voltage on the capillary: 5500 V for positive mode, -4500 V for negative mode, declastering potential: 90 V. Mass-spectra were recorded in m/z range 150 – 3000, accumulation time 250 ms.

Purity of the compounds was assessed using HPLC-DAD-MS. HPLC-DAD-MS system consisting of a Vanquish liquid chromatograph (Thermo Fisher Scientific, USA) and an Orbitrap Fusion Lumos Tribrid (Thermo Fisher Scientific, USA) mass spectrometer was used. A Shim-pack GIST C18-Aq liquid chromatography reversed-phase column (3 x 150 mm, 3 μm, Shimadzu, Japan) was used.

HPLC-DAD-MS system consisting of a Vanquish liquid chromatograph (Thermo Fisher Scientific, USA) and an Orbitrap Fusion Lumos Tribrid (Thermo Fisher Scientific, USA) mass spectrometer was used. A Shim-pack GIST C18-Aq liquid chromatography reversed-phase column (3 x 150 mm, 3 μm, Shimadzu, Japan) was used.

HPLC-HRMS analysis was performed with Vanquish liquid chromatograph (Thermo Fisher Scientific, USA) and a high-resolution mass spectrometer based on the G3 QTof quadrupole-time-of-flight (Waters, USA) equipped with an electrospray ionization source (ESI) was used.

To separate the components of the analyzed solution, a Shim-pack GIST C18-Aq chromatographic column (3 x 150 mm, 3 μm, Shimadzu, Japan) filled with a reverse-phase sorbent with polar-endcapping was used. The column temperature was maintained at 35 °C throughout the analysis using a thermostat. A 0.1% aqueous solution of formic acid (A) and acetonitrile

(B) were used as eluents. An isocratic elution mode was used with a ratio of eluents A and B of 15:85%. The flow rate of the mobile phase was 0.4 ml/min. The injected sample volume was 1.0 µl. The analysis time was 10 minutes. The ESI-MS conditions on the Orbitrap Fusion Lumos Tribrid were as follows: mode for recording positively and negatively charged molecules; the capillary voltage of the ionization source was 3500 V for the positive mode and -2500 V for the negative mode; ion source chamber temperature - 350 °C; ion transfer interface temperature - 325 °C; gas pressure for solvent atomization in the ion source (nitrogen) - 50, auxiliary gas pressure - 10, curtain gas pressure - 1. Scanning range m/z: 200-1700 Da. The resolution of the mass spectrometer for analysis is not less than 15000. The mass spectrometer was calibrated immediately prior to sample analysis using CalMix PierceTM calibration mixtures (Thermo Scientific, USA). Data processing was performed using Xcalibur 4.6 software (Thermo Scientific, USA).

ICP-MS. Determination of Pt concentration was carried out with a quadrupole ICP-MS spectrometer PlasmaQuant MS Elit (AnalytikJena, Germany). The data were acquired and processed with the ASpect MS software package (version 4.3, AnalytikJena). ICP-MS procedure included determining of following isotopes: ^{195}Pt as the analyte and ^{175}Lu as the internal standard (the concentration of Lu 1 µg L^{-1}).

The ICP-MS-68A-C multi-element standard solution (High-Purity Standards, USA), containing 10 mg L^{-1} Ru, Rh, Pd, Os, Ir, Pt and Au, was used to prepare calibration solutions (0.2, 0.5, 1, 2, 5, 10, 20 µg L^{-1}). A single-element solution of lutetium (1 g L^{-1}) was obtained by dissolution of lutetium oxide. All solutions were prepared using deionized water (18.2 MΩ cm, Millipore, France).

Temperature monitoring was conducted using the IR camera Gobi-384-GigE (Envision Xenics, Belgium). The recorded objects were placed at 25 cm from the camera to place them in focus of the camera. Data was recorded in an unaltered configuration at 10 fps, the obtained images were processed in the Xeneth software v.2.6.0.309. For *in vitro* experiments, the unaffected by NIR light part of the surrounding room was used as a reference temperature of the environment.

Dynamic light scattering (DLS) and zeta-potential measurements were performed using Zetasizer Nano ZS device (Malvern Pananalytical, Malvern, Worcestershire, UK) at 25 °C. Each measurement was performed in triplicate. DLS analysis was performed in backscatter mode (173°), and the results are reported as intensity-based distributions**.**

Atomic force microscopy (AFM) measurements for **C_6F_5-Pt-F127-NPs** and **NO_2-Pt-NPs** were performed in air using a NTEGRA II microscope (NT-MDT SI, Russia) in semi-contact mode with silicon cantilevers (1.74 N/m, 90 kHz). AFM measurements for **C_6F_5-Pt-DSPE-NPs** and **NO_2-Est-NPs** were performed in air using a NTEGRA Prima II microscope (NT-MDT SI, Russia) in semi-contact mode with HA-CNC cantilevers (1 N/m, 46kHz).

Transmission electron microscopy (TEM). The morphology of J-aggregates was studied using a JEOL JEM-1400 (120 kV) transmission electron microscope. 10 µL of colloidal solution of J-aggregates was dropped onto the surface of a Formvar-coated copper grid, and the solvent was subsequently evaporated before analyzing at room temperature. No additional contrasts were used. **C_6F_5-Pt** (99% H2O) was used to study CT-coupled aggregates. To study slipped-stacked J-aggregates, **C_6F_5-Pt** (1 mg/ml in acetone) was diluted to 30% acetone, incubated for 1 minute and then diluted with water prior to dropping on the copper grid.

Photoreduction studies of NO_2-Pt and C_6F_5-Pt. All experiments were carried out at room temperature. Pt(IV) prodrugs NO2-Pt and C6F5-Pt were dissolved in a mixture of MeOH:DMSO:H2O (6:3:1, v/v/v) to the resulting concentration of 10-3 M. The 1 mM solutions of NO2-Pt and C6F5-Pt in a transparent vial (d = 1 cm) were placed in front of the light source (λ= 660 nm) so that irradiation power density was equal to 13.5 mW/cm^2.

In all experiments a 30 ml aliquot of the Pt(IV) prodrugs solution was taken and adjusted with MeOH to 500 ml at different time points (0, 2, 5, 10, 20, 40, 60 min). HPLC-MS-analysis of the probes was performed and repeated two times each. An amount of cisplatin-adduct in the probes was calculated from the peak area on the chromatogram. Changes in the levels of the compound of interest within the experiment were investigated by integrating the peaks of the $Pt(NH_3)_2Cl(C_2H_6SO)$ ion in the range m/z 340.5-345.5 Da.

2. Synthesis and characterization of monomers

Scheme S1. Synthesis of **C_6F_5-Pt, C_6F_5-Est**, **NO_2-Pt** and **NO_2-Est**.

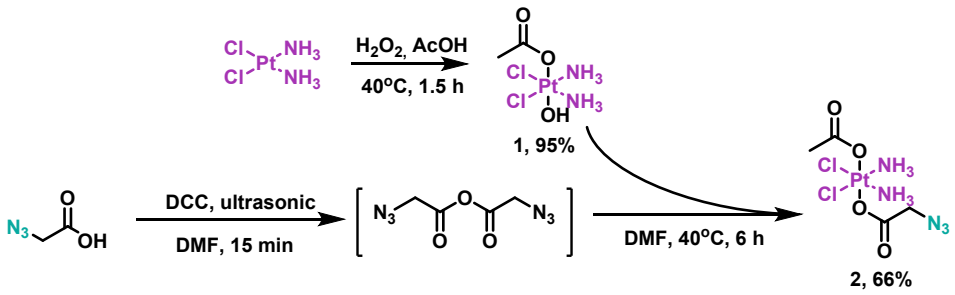

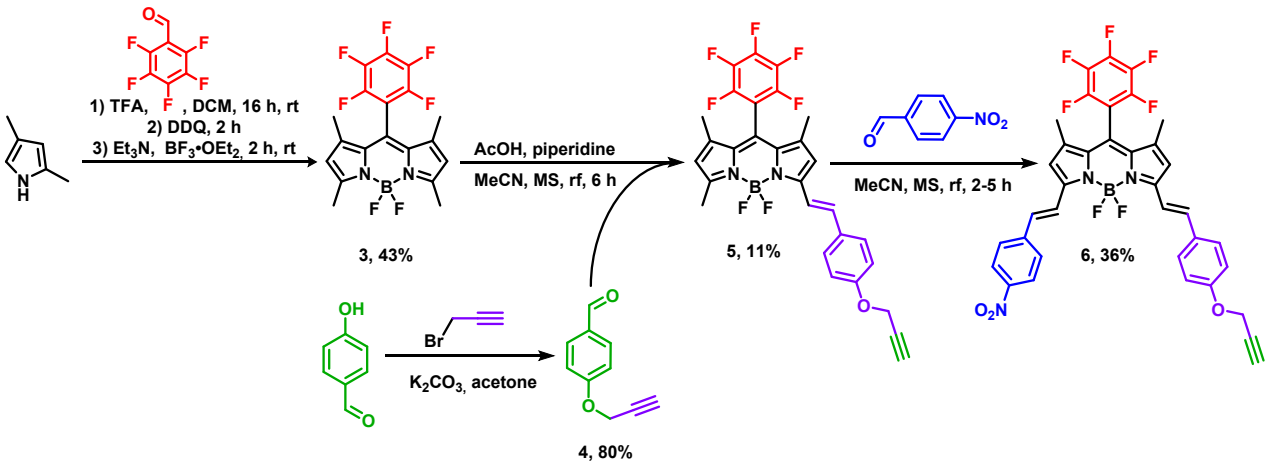
1) TFA, , DCM, 16 h, rt
2) DDQ, 2 h
3) Et3N, BF3•OEt2, 2 h, rt
3, 43%
AcOH, piperidine
MeCN, MS, rf, 6 h
5, 11%
MeCN, MS, rf, 2-5 h
6, 36%
K2CO3, acetone
4, 80%

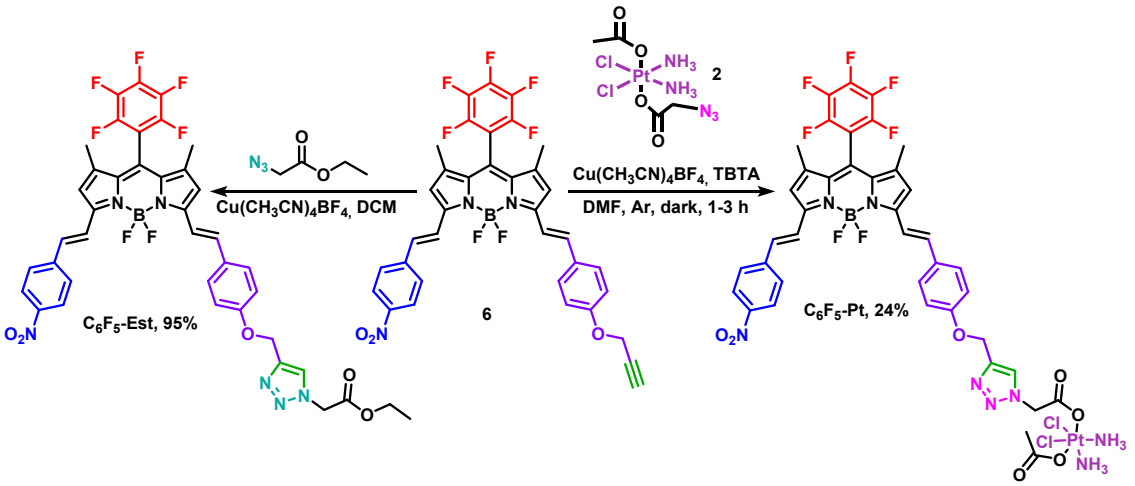
Cu(CH3CN)4BF4, DCM
C6F5-Est, 95%
6
Cu(CH3CN)4BF4, TBTA
DMF, Ar, dark, 1-3 h
C6F5-Pt, 24%
2

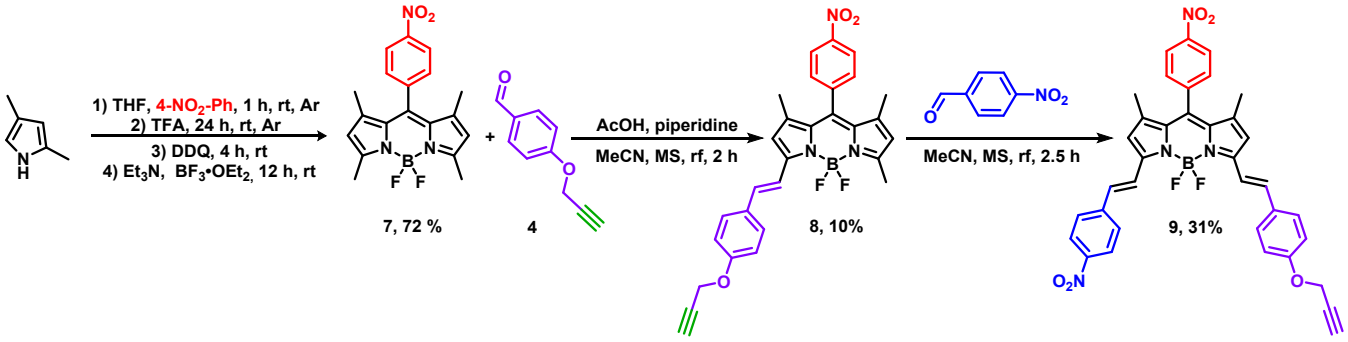
1) THF, 4-NO2-Ph, 1 h, rt, Ar
2) TFA, 24 h, rt, Ar
3) DDQ, 4 h, rt
4) Et3N, BF3•OEt2, 12 h, rt
7, 72 %
4
AcOH, piperidine
MeCN, MS, rf, 2 h
8, 10%
MeCN, MS, rf, 2.5 h
9, 31%

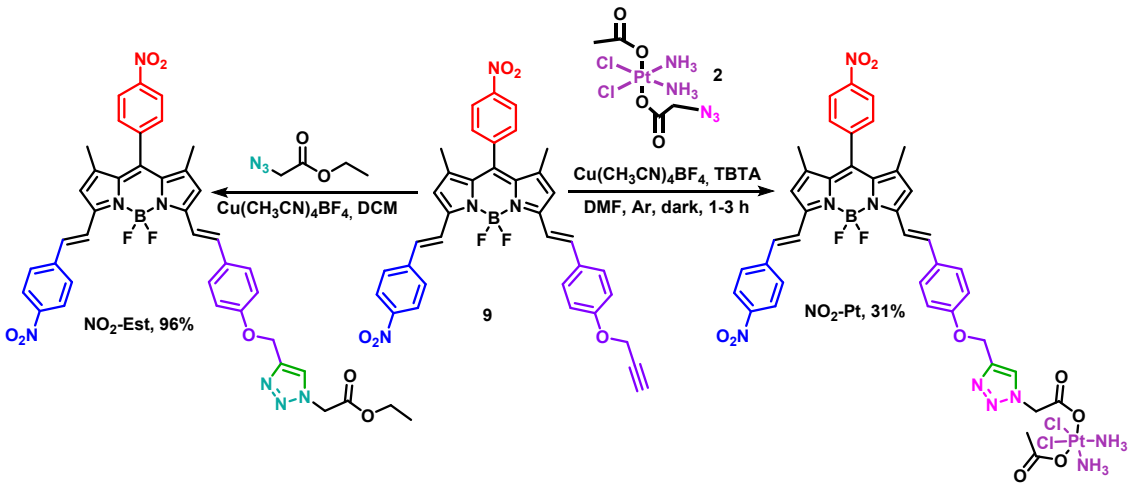
Cu(CH3CN)4BF4, DCM
NO2-Est, 96%
9
Cu(CH3CN)4BF4, TBTA
DMF, Ar, dark, 1-3 h
NO2-Pt, 31%
2

[OC-6-44]-Acetatodiamminedichloridohydroxidoplatinum(IV) 1 was synthesized according to previous reports.[2] 100 mg (0.334 mmol) of cisplatin was dissolved in 40 ml of glacial acetic acid and 1.73 ml of H_2O_2 (30% w/w) was added. The reaction mixture was stirred for 2 hours at 35–40°C until the precipitate dissolved and the solution became transparent. Then, the solution was concentrated under reduced pressure to 3-4 ml. The excess (30 ml) diethyl ether was added and the resulting suspension was centrifuged. The precipitate was separated and washed with diethyl ether, then it was left to dry on air. Compound **1** was obtained as a white powder. Yield: 119 mg (95%).
^{1}H NMR (400 MHz, DMSO-d_6, δ, ppm.): 6.13 – 5.78 (m, 6H, NH_3), 1.87 (s, 3H, CH_3)

[Pt(OAc)(2-azidoacetate)(Cl_2(NH_3)$_2$)] 2 was synthesized according to previous reports.[2] 266 mg (1.29 mmol, 4 equiv.) of DCC was dissolved in 6 ml of DMF and 130 mg (1.29 mmol, 4 equiv.) of 2-azidoacetic acid was added. The reaction mixture was suspended in an ultrasonic bath for 15 min. Then, the formed precipitate was separated by centrifugation. The resulting solution of 2-azidoacetic anhydride in DMF was mixed with suspension of 121 mg (0.32 mmol, 1 equiv.) of compound **1** in 4.5 ml of DMF. The reaction mixture was stirred at r.t. overnight and then at 40°C for 6 hours. After that, the solution was removed under reduced pressure and the crude product was suspended in 0.5 ml of MeOH and precipitated by addition of diethyl ether. The precipitate was separated by centrifugation and was purified by flash chromatography using CH_2Cl_2:MeOH = 10:1 as eluent. Compound **2** was obtained as a light yellow powder. Yield: 98 mg (66%).
^{1}H NMR (400 MHz, DMSO-d_6, δ, ppm.): 6.88 – 6.20 (m, 6H, NH_3), 3.89 (s, 2H, C(O)CH_2N_3), 1.92 (s, 3H, C(O)-CH_3).

5,5-difluoro-1,3,7,9-tetramethyl-10-(perfluorophenyl)-5*H*-4λ^4,5λ^4-dipyrrolo[1,2-*c*:2',1'-*f*][1,3,2]diazaborinine 3. BODIPY **3** was synthesized according to previous reports[3] with slight modifications. Pentafluorobenzaldehyde (429 mg, 2.19 mmol) and 2,4-dimethyl-1*H*-pyrrole (500 µl, 4.86 mmol) were dissolved in DCM (172 ml) under argon atmosphere, then TFA (18 µl) was added and the mixture was stirred at room temperature (r.t.). After 4 h stirring 2,3-dichloro-5,6-dicynao-1,4-benzoquinone (DDQ) (1192 mg, 5.25 mmol) was added. The reaction was allowed to proceed for 4 h at r.t. The reaction mixture was then cooled in an ice-water bath, Et_3N (5.15 ml) and $BF_3{\cdot}Et_2O$ (5.15 ml)
were added dropwise. The resulting mixture was kept stirring at r.t. overnight, then washed with H_2O and extracted with DCM. The combined organic layers were dried over anhydrous Na_2SO_4 and evaporated under reduced pressure. The crude product was purified by silica gel column chromatography (DCM : Petroleum ether = 1:1). BODIPY **3** was obtained as a red powder. Yield: 390 mg (43 %).
^{1}H NMR (400 MHz, $CDCl_3$, δ, ppm): 6.06 (s, 1H, 2,6-BP), 2.57 (s, 6H, 3,5-Me), 1.62 (s, 6H, 1,7-Me).

4-(prop-2-yn-1-yloxy)benzaldehyde 4. *p*-hydroxybenzaldehyde (10 g, 1 equiv.), propargyl bromide (14.03 ml, 2 equiv.) and K_2CO_3 (22.62 g, 2 equiv.) were dissolved in 340 ml of acetone. The reaction mixture was washed with brine and extracted with CH_2Cl_2. The combined organic layers were dried over anhydrous Na_2SO_4 and evaporated under reduced pressure. The crude product was purified by flash chromatography (CH_2Cl_2). Aldehyde **4** was obtained as a white powder. Yield: 13.11 g (quantitative yield).
^{1}H NMR (400 MHz, $CDCl_3$, δ, ppm): 9.91 (s, 1H, CHO), 7.88 – 7.84 (m, 2H, 2,6-Ph), 7.13 – 7.05 (m, 2H, 3,5-Ph), 4.78 (d, *J* = 2.4 Hz, 2H, CH2), 2.57 (t, *J* = 2.4 Hz, 1H, CH).

(*E*)-5,5-difluoro-1,3,9-trimethyl-10-(perfluorophenyl)-7-(4-(prop-2-yn-1-yloxy)styryl)-5*H*-4λ^4,5λ^4-dipyrrolo[1,2-*c*:2',1'-*f*][1,3,2]diazaborinine 5. To a stirred solution of BODIPY **3** (278 mg, 0.67 mmol) and aldehyde **4** (131 mg, 0.61 mmol) in 18 ml of MeCN 20 µl of piperidine, 10 µl of acetic acid and 0.7 g of 3 Å molecular sieves were added. The reaction mixture was then refluxed for 2 hours with the progress of the reaction monitored by thin-layer chromatography (TLC). Following this, the solvent was evaporated under reduced pressure, and the residue purified by silica gel column chromatography (CH_2Cl_2 : Petroleum ether = 1:1). The BODIPY **5** was obtained as a red powder. Yield: 41 mg (11%).
^{1}H NMR (400 MHz, $CDCl_3$, δ, ppm): 7.61 – 7.51 (m, 3H, H=2, 5, 1), 7.26 (d, *J* = 16.4 Hz, 1H, H=1'), 7.00 (d, *J* = 8.7 Hz, 2H, H=3, 4), 6.67 (s, 1H, H=2-BP), 6.07 (s, 1H, H=6-BP), 4.74 (d, *J* = 2.4 Hz, 2H, H=CH_2), 2.61 (s, 3H, H=3-Me), 2.55 (t, *J* = 2.4 Hz, 1H, H=CH), 1.67 (s, 3H, H=1-Me), 1.63 (m, 3H, H=7-Me).
HRMS: calc. for $C_{29}H_{21}BF_7N_2O^+$ (**5**+H)$^+$, 557.1635; found $C_{29}H_{21}BF_7N_2O^+$ (**5**+H)$^+$, 557.1622.

5,5-difluoro-1,9-dimethyl-3-((*E*)-4-nitrostyryl)-10-(perfluorophenyl)-7-((E)-4-(prop-2-yn-1-yloxy)styryl)-5*H*-4λ^4,5λ^4-dipyrrolo[1,2-*c*:2',1'-*f*][1,3,2]diazaborinine 6. To a stirred solution of BODIPY **5** (78 mg, 0.14 mmol) and 4-Nitrobenzaldehyde (21 mg, 0.14 mmol) in 13 ml of MeCN 20 µl of piperidine, 10 µl of acetic acid and 1 g of 3 Å molecular sieves were added. The reaction mixture was then refluxed for 3 hours with the progress of the reaction monitored by thin-layer chromatography (TLC). Following this, the solvent was evaporated under reduced pressure, and the residue purified by silica gel column chromatography (CH_2Cl_2 : Petroleum ether = 2:1). The BODIPY **6** was obtained as a dark blue powder. Yield: 35 mg (36 %).
^{1}H NMR (400 MHz, $CDCl_3$, δ, ppm): 8.26 (d, *J* = 8.8 Hz, 2H, H=3, 4), 7.84 (d, *J* = 16.3 Hz, 1H, H=1'), 7.74 (d, *J* = 8.7 Hz, 2H, H=2, 5), 7.67 – 7.59 (m, 3H, H=2', 5', 1), 7.36 (d, *J* = 16.2 Hz, 1H, H=1a), 7.25 (d, *J* = 16.0 Hz, 1H, H=1a'), 7.05 (d, *J* = 8.6 Hz, 2H, H=3', 4'), 6.77 (s, 1H, H=6-BP), 6.72 (s, 1H, H=2-BP), 2.57 (t, *J* = 2.4 Hz, 1H, H=CH), 1.71 (s, 3H, H=7-Me), 1.70 (s, 3H, H=1-Me).
HRMS: calc. for $C_{36}H_{23}BF_7N_3NaO_3^+$ (**6**+Na)$^+$ 712.1618; found $C_{36}H_{23}BF_7N_3NaO_3^+$ (**6**+Na)$^+$ 712.1622.

ethyl 2-(4-((4-((*E*)-2-(5,5-difluoro-1,9-dimethyl-7-((E)-4-nitrostyryl)-10-(perfluorophenyl)-5*H*-4λ^4,5λ^4-dipyrrolo[1,2-*c*:2',1'-*f*][1,3,2]diazaborinin-3-yl)vinyl)phenoxy)methyl)-1H-1,2,3-triazol-1-yl)acetate C_6F_5-Est. BODIPY **6** (23.4 mg, 0.034 mmol) and ethyl 2-azidoacetate (8.8 mg, 0.068 mmol) were dissolved in 3 ml of CH_2Cl_2 and $Cu(CH_3CN)_4{\bullet}BF_4$ (5.3 mg, 0.017 mmol) was added under argon atmosphere. The reaction mixture was stirred for 2 hours at r.t. The solvent was evaporated under reduced pressure, and the residue was purified by silica gel column chromatography (CH_2Cl_2). **C_6F_5-Est** was obtained as a dark blue powder. Yield: 27 mg (96%).

^{1}H NMR (400 MHz, $CDCl_3$) δ 8.26 (d, *J* = 8.7 Hz, 2H, H=3, 4), 7.84 (d, *J* = 16.5 Hz, 1H, H=1'), 7.80 (s, 1H, H=CH), 7.74 (d, *J* = 8.7 Hz, 2H, H=2, 5), 7.65 – 7.57 (m, 3H, H=2', 5', 1), 7.35 (d, *J* = 16.2 Hz, 1H, H=1a), 7.26 (d, 1H, H=1a'), 7.06 (d, *J* = 8.7 Hz, 2H, H=3', 4'), 6.76 (s, 1H, H=6-BP), 6.72 (s, 1H, H=2-BP), 5.32 (s, 2H, H=N-CH_2), 5.19 (s, 2H, H=CH_2), 4.29 (q, *J* = 7.2 Hz, 2H, H=O-CH_2), 1.71 (s, 3H, H=7-Me), 1.69 (s, H=1-Me), 1.31 (t, *J* = 7.1 Hz, 3H, H=CH_3).
HRMS: calc. for $C_{40}H_{31}BF_7N_6O_5^+$ (C_6F_5-Est +H)$^+$ 819.2337; found $C_{40}H_{31}BF_7N_6O_5^+$ (C_6F_5-Est +H)$^+$, 819.2330.

C_6F_5-Pt. BODIPY **6** (35 mg, 0.05 mmol) was dissolved in 1.1 ml of DMF and $Cu(CH_3CN)_4$•BF_4 (3.9 mg, 12 μmol), TBTA (8 mg, 15 μmol) were added under argon atmosphere. The reaction mixture was stirred for 15 min at r.t., complex **2** (19 mg, 0.041 mmol) was added and the solution was stirred for another 2 hour at r.t. The solvent was evaporated under reduced pressure. The residue was purified by column chromatography (CH_2Cl_2:MeOH = 10:1). Complex **C_6F_5-Pt** was obtained as a dark green powder. Yield: 11 mg (24%).
^{1}H NMR (400 MHz, $CDCl_3$, δ, ppm): 8.31 (d, *J* = 8.8 Hz, 2H, H=3, 4), 8.16 (s, 1H, H=CH), 7.88 (d, *J* = 8.7 Hz, 2H, H=2, 5), 7.81 (d, *J* = 15.9 Hz, 1H, H=1'), 7.74 (d, *J* = 16.2 Hz, 1H, H=1), 7.71 – 7.63 (m, 3H, H=1a, 2', 5'), 7.44 (d, *J* = 16.2 Hz, 1H, H=1a'), 7.24 – 7.17 (m, 3H, H=3', 4', 6-BP), 7.12 (s, 1H, 2-BP), 6.52 (br.s, 6H, H=NH_3), 5.26 (s, 2H, H=N-CH_2), 5.24 (s, 2H, H=CH_2), 1.92 (s, 3H, H=CH_3), 1.74 (s, 3H, H=7-Me), 1.72 (s, 3H, H=1-Me).
HRMS: calc. for $C_{40}H_{35}BCl_2F_7N_8O_7Pt^+$ (**C_6F_5-Pt**+H)$^+$, 1149.1584; found $C_{40}H_{35}BCl_2F_7N_8O_7Pt^+$ (**C_6F_5-Pt**+H)$^+$, 1149.1583.

5,5-difluoro-1,3,7,9-tetramethyl-10-(4-nitrophenyl)-5*H*-4λ^4,5λ^4-dipyrrolo[1,2-*c*:2',1'-*f*][1,3,2]diazaborinine 7. BODIPY **7** was synthesized according to previous reports[4] with slight modifications. 4-Nitrobenzaldehyde (187 mg, 1.24 mmol) and 2,4-dimethyl-1*H*-pyrrole (281 μl, 2.74 mmol) were dissolved in THF (37 ml) under argon atmosphere, after 1 h of stirring TFA (20 μl) was added and the mixture was stirred at r.t. After 24 h stirring DDQ (364 mg, 1.6 mmol) in dry THF (41 ml) was added drop by drop. The reaction was allowed to proceed for 5 h at r.t. The reaction mixture was then cooled in an ice-water bath, Et_3N (7.4 ml) and BF_3·Et_2O (7.4 ml) were added dropwise. The resulting mixture was kept stirring at r.t. overnight, then it was filtered. The solid obtained was washed with THF, acetone and DCM. The organic phases were concentrated under reduced pressure. Then the residue was dissolved in DCM, washed with saturated $NaHCO_3$ and water. The organic phase was dried over anhydrous Na_2SO_4 and evaporated under reduced pressure. The crude product was purified by silica gel column chromatography (DCM : Petroleum ether = 1:1). BODIPY **7** was obtained as an orange-red powder. Yield: 318 mg (70 %).
^{1}H NMR (400 MHz, $CDCl_3$, δ, ppm): 8.40 (m, 2H, H=2,6-Ph), 7.55 (m, 2H, H=3,5-Ph), 6.02 (s, 2H, H=2,6-BP), 2.58 (s, 6H, H=3,5-Me), 1.37 (s, 6H, H=1,7-Me).

(*E*)-5,5-difluoro-1,3,9-trimethyl-10-(4-nitrophenyl)-7-(4-(prop-2-yn-1-yloxy)styryl)-5*H*-4λ^4,5λ^4-dipyrrolo[1,2-*c*:2',1'-*f*][1,3,2]diazaborinine 8. To a stirred solution of BODIPY **7** (343 mg, 0.93 mmol) and aldehyde **4** (134 mg, 0.84 mmol) in 29 ml of MeCN 20 μl of piperidine, 10 μl of acetic acid and 0.81 g of 3 Å molecular sieves were added. The reaction mixture was then refluxed for 3 hours with the progress of the reaction monitored by thin-layer chromatography (TLC). Following this, the solvent was evaporated under reduced pressure, and the residue purified by silica gel column chromatography (CH_2Cl_2 : Petroleum ether = 1:1). The BODIPY **8** was obtained as a violet powder. Yield: 47 mg (10%).
^{1}H NMR (400 MHz, $CDCl_3$, δ, ppm): 8.39 (d, *J* = 8.5 Hz, 2H, H=2,6-Ph), 7.56 (m, 5H, H=3,5-Ph, 2, 5, 1), 7.23 (d, *J* = 17.1 Hz, 1H, H=1'), 6.99 (d, *J* = 8.6 Hz, 2H, H=3, 4), 6.62 (s, 1H, H=6-BP), 6.03 (s, 1H, H=2-BP), 4.74 (d, *J* = 2.4 Hz, 2H, H=CH_2), 2.60 (s, 3H, H=5-Me), 2.55 (t, *J* = 2.2 Hz, 1H, H=CH), 1.41 (s, 3H, H=1-Me), 1.37 (s, 3H, H=7-Me).

5,5-difluoro-1,9-dimethyl-10-(4-nitrophenyl)-3-((*E*)-4-nitrostyryl)-7-((E)-4-(prop-2-yn-1-yloxy)styryl)-5*H*-4λ^4,5λ^4-dipyrrolo[1,2-*c*:2',1'-*f*][1,3,2]diazaborinine 9. To a stirred solution of BODIPY **8** (53 mg, 0.1 mmol) and 4-Nitrobenzaldehyde (16 mg, 0.1 mmol) in 8 ml of MeCN 20 μl of piperidine, 10 μl of acetic acid and 0.74 g of 3 Å molecular sieves were added. The reaction mixture was then refluxed for 3 hours with the progress of the reaction monitored by thin-layer chromatography (TLC). Following this, the solvent was evaporated under reduced pressure, and the residue purified by silica gel column chromatography (Acetone : Petroleum ether = 1:3). The BODIPY **9** was obtained as a dark blue powder. Yield: 21 mg (31 %).
^{1}H NMR (400 MHz, $CDCl_3$, δ, ppm): 8.42 (d, *J* = 8.3 Hz, 2H, H=2,6-Ph), 8.26 (d, *J* = 8.4 Hz, 2H, H=3,4), 7.85 (d, *J* = 16.4 Hz, 1H, H=1'), 7.74 (d, *J* = 8.6 Hz, 2H, H=3,5-Ph), 7.62 (m, 5H, H=2,5, 2', 5', 1), 7.33 (d, *J* = 16.1 Hz, 1H, H=1a), 7.21 (s, 1H, H=1a'), 7.05 (d, *J* = 8.5 Hz, 2H, H=3',4'), 6.72 (s, 1H, H=6-BP), 6.68 (s, 1H, H=2-BP), 4.77 (d, *J* = 2.5 Hz, 2H, H=CH_2), 2.60 – 2.55 (m, 1H, H=CH), 1.46 (s, 3H, H=7-Me), 1.44 (s, 3H, H=1-Me).
HRMS: calc. for $C_{36}H_{27}BF_2N_4NaO_5^+$ (**9**+Na)$^+$ 667.1940; found $C_{36}H_{27}BF_2N_4NaO_5^+$ (**9**+Na)$^+$ 667.1946.

ethyl 2-(4-((4-((E)-2-(5,5-difluoro-1,9-dimethyl-10-(4-nitrophenyl)-7-((*E*)-4-nitrostyryl)-5*H*-4λ^4,5λ^4-dipyrrolo[1,2-*c*:2',1'-*f*][1,3,2]diazaborinin-3-yl)vinyl)phenoxy)methyl)-1H-1,2,3-triazol-1-yl)acetate NO_2-Est. BODIPY **9** (26.4 mg, 0.041 mmol) and ethyl 2-azidoacetate (10.6 mg, 0.082 mmol) were dissolved in 4.8 ml of CH_2Cl_2 and $Cu(CH_3CN)_4$•BF_4 (6.4 mg, 0.021 mmol) was added under argon atmosphere. The reaction mixture was stirred for 2 hours at r.t. The solvent was evaporated under reduced pressure, and the residue was purified by silica gel column chromatography (CH_2Cl_2). **NO_2-Est** was obtained as a dark blue powder. Yield: 30 mg (95%).
^{1}H NMR (400 MHz, $CDCl_3$, δ, ppm): 8.42 (d, *J* = 8.6 Hz, 2H, 2,6-Ph), 8.26 (d, *J* = 8.7 Hz, 2H, H=3,4), 7.85 (d, *J* = 16.2 Hz, 1H, H=1'), 7.81 (s, 1H, H=CH), 7.74 (d, *J* = 8.7 Hz, 2H, H=3,5-Ph), 7.61 (m, *J* = 8.8, 3.4 Hz, 5H, H=2,5, 2', 5', 1), 7.32 (d, *J* = 16.2 Hz, 1H, H=1a), 7.23 (d, *J* = 16.5 Hz, 1H, H=1a'), 7.06 (d, *J* = 8.7 Hz, 2H, H=3',4'), 6.71 (s, 1H, H=6-BP), 6.68 (s, 1H, H=2-BP), 4.69 (s, 4H, H=CH_2, N-CH_2), 4.29 (q, *J* = 7.2 Hz, 2H, H=O-CH_2), 1.45 (s, 3H, H=7-Me), 1.44 (s, 3H, H=1-Me), 1.31 (t, *J* = 7.2 Hz, 3H, H=CH_3).

NO_2-Pt. BODIPY **6** (42 mg, 0.065 mmol) was dissolved in 3 ml of DMF and $Cu(CH_3CN)_4 \bullet BF_4$ (6.1 mg, 19.6 μmol), TBTA (10.4 mg, 19.6 μmol) were added under argon atmosphere. The reaction mixture was stirred for 15 min at r.t., complex **2** (30 mg, 0.065 mmol) was added and the solution was stirred for another 2 hour at r.t. The solvent was evaporated under reduced pressure. The residue was purified by column chromatography (CH_2Cl_2:MeOH = 10:1). Complex **NO_2-Pt** was obtained as a dark green powder. Yield: 22 mg (31%).
^{1}H NMR (400 MHz, $CDCl_3$, δ, ppm): 8.43 (d, *J* = 8.5 Hz, 2H, 2,6-Ph), 8.31 (d, *J* = 8.6 Hz, 2H, H=3,4), 8.16 (s, 1H, H=CH), 7.85 (m, 4H, H=1, 1', 3,5-Ph), 7.75 – 7.62 (m, 5H, H=2, 5, 2', 5', 1a), 7.45 (d, *J* = 16.2 Hz, 1H, H=1a'), 7.19 (d, *J* = 8.4 Hz, 2H, H=3',4'), 7.11 (s, 1H, H=6-BP), 7.04 (s, 1H, H=2-BP), 6.52 (br. s, 6H, H=NH_3), 5.25 (s, 2H, N-CH_2), 5.24 (s, 2H, H=CH_2), 1.92 (s, 3H, H=CH_3), 1.45 (s, 3H, H=7-Me), 1.42 (s, 3H, H=1-Me).
^{13}C NMR (101 MHz, DMSO-d_6, δ, ppm): 78.13, 173.32, 159.78, 155.45, 149.34, 148.14, 146.88, 143.42, 142.76, 142.11, 140.83, 140.06, 139.55, 136.28, 133.24, 133.13, 130.51, 129.38, 127.90, 127.74, 126.03, 124.42, 124.35, 122.11, 119.76, 118.81, 115.54, 61.31, 50.57, 22.66, 14.79, 14.47.
HRMS: calc. for $C_{40}H_{38}BCl_2F_2N_9NaO_9Pt^+$ (**NO_2-Pt**+Na)$^+$ 1126.1778; found $C_{40}H_{38}BCl_2F_2N_9NaO_9Pt^+$ (**NO_2-Pt**+Na)$^+$ 1126.1773.

2. Structural Characterization and Purity Analysis (NMR, HRMS and RP-HPLC analysis)

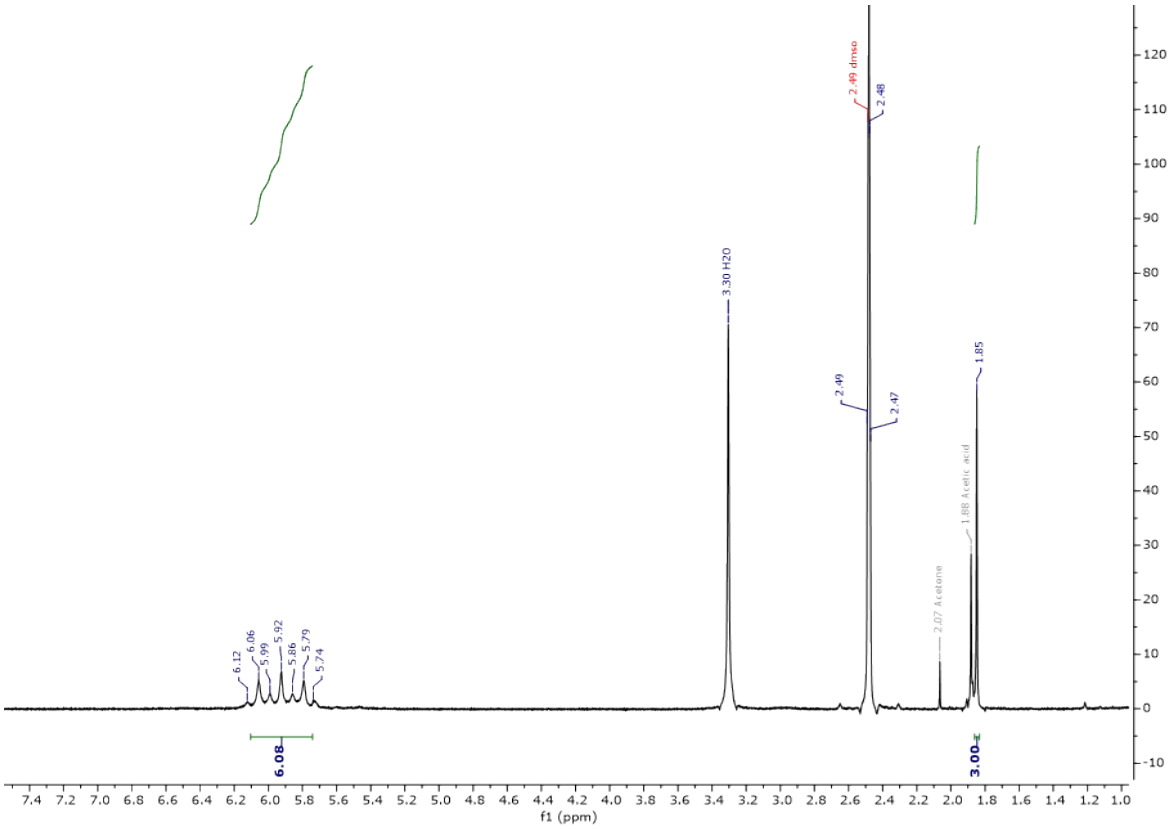

Figure S1. ^{1}H NMR-spectrum of [OC-6-44]-Acetatodiamminedichloridohydroxidoplatinum(IV) **1** in DMSO-d_6.

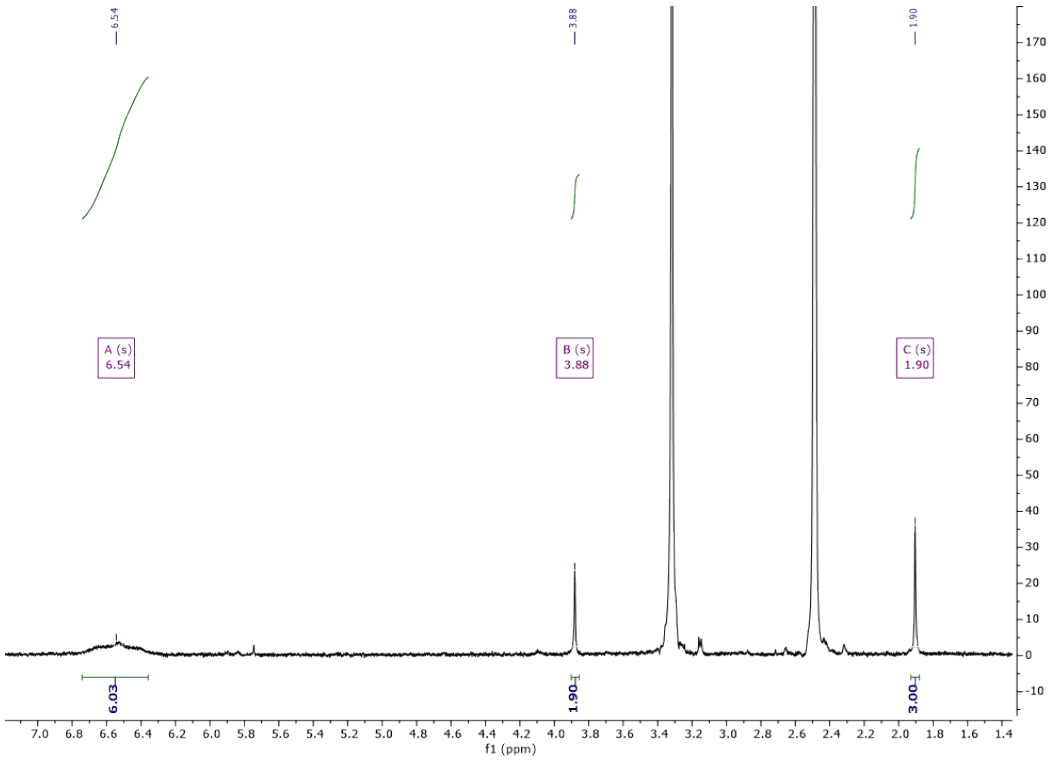

Figure S2. ^{1}H NMR-spectrum of [Pt(OAc)(2-azidoacetate)(Cl_2(NH_3)$_2$)] **2** in DMSO-d_6.

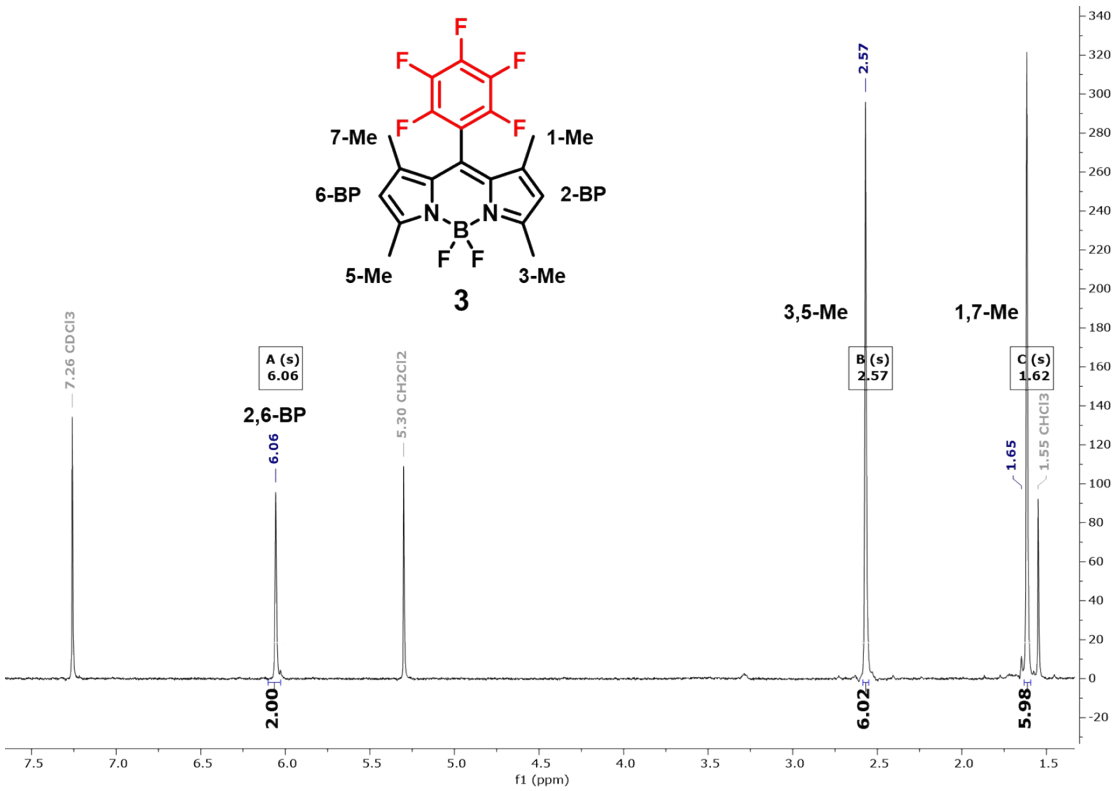

Figure S3. ^{1}H NMR-spectrum of 5,5-difluoro-1,3,7,9-tetramethyl-10-(perfluorophenyl)-5*H*-4λ^4,5λ^4-dipyrrolo[1,2-*c*:2',1'-*f*][1,3,2]diazaborinine **3** in $CDCl_3$.

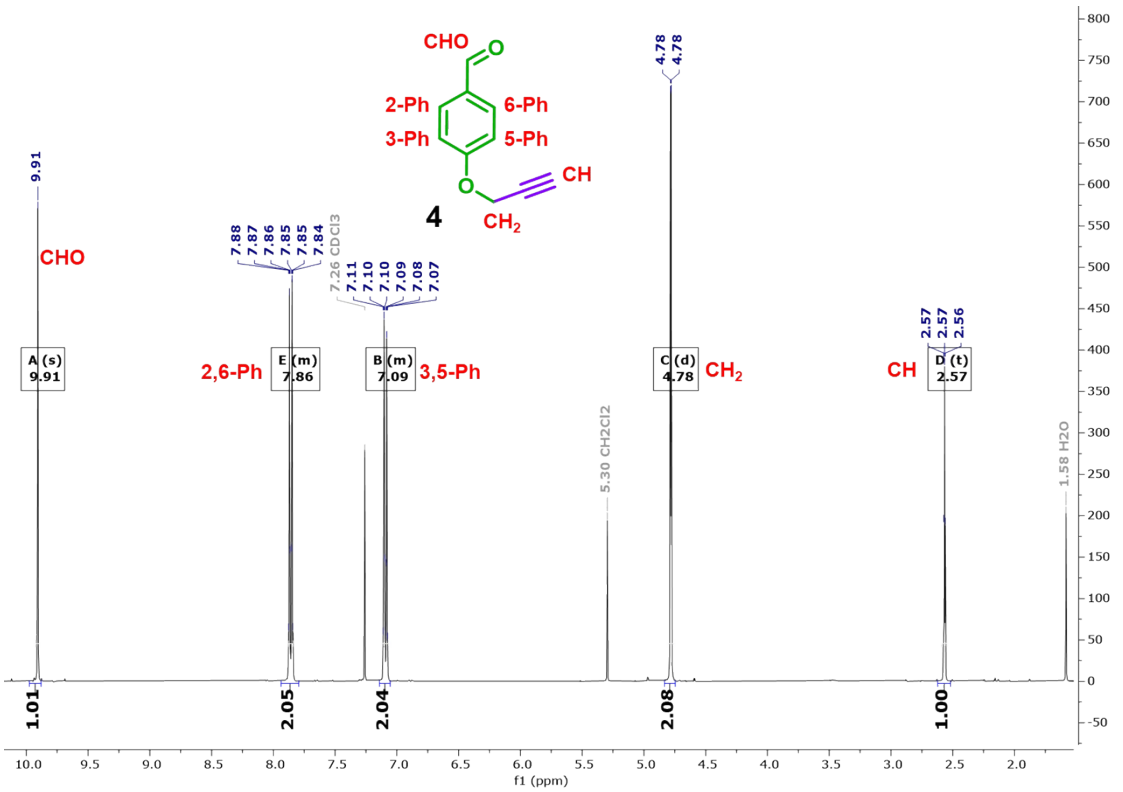

Figure S6. ^{1}H NMR-spectrum of 4-(prop-2-yn-1-yloxy)benzaldehyde **4** in $CDCl_3$.

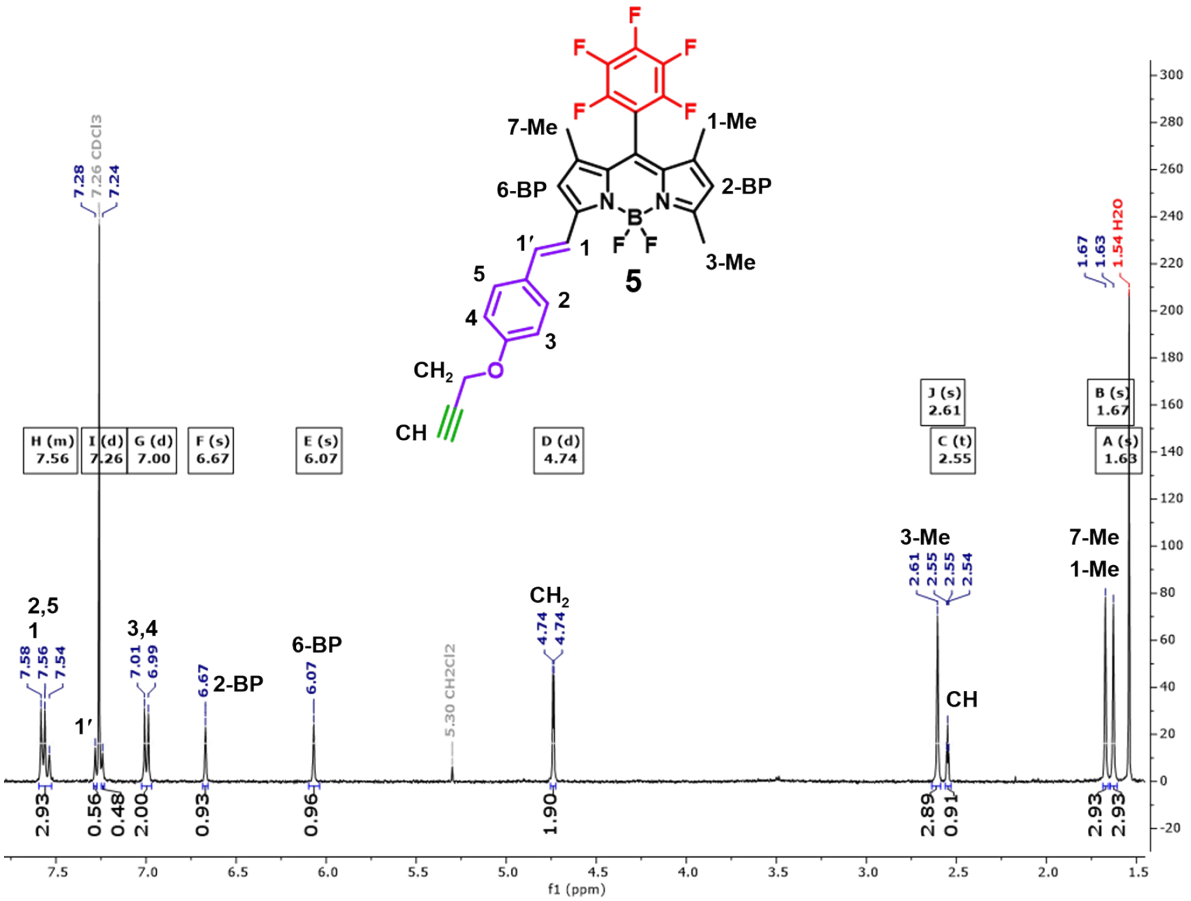

Figure S7. ^{1}H NMR-spectrum of (*E*)-5,5-difluoro-1,3,9-trimethyl-10-(perfluorophenyl)-7-(4-(prop-2-yn-1-yloxy)styryl)-5*H*-4λ^{4},5λ^{4}-dipyrrolo[1,2-*c*:2',1'-*f*][1,3,2]diazaborinine **5** in $CDCl_3$.

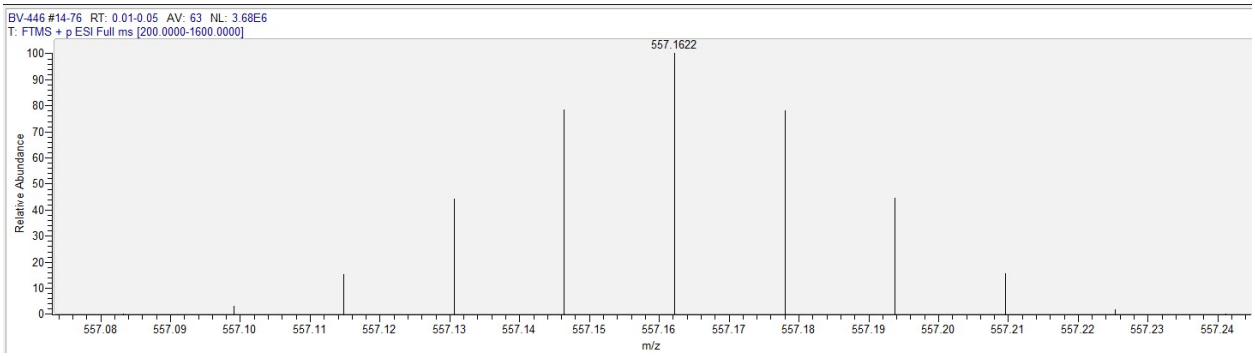

Figure S8. ESI-high resolution mass spectrum of (*E*)-5,5-difluoro-1,3,9-trimethyl-10-(perfluorophenyl)-7-(4-(prop-2-yn-1-yloxy)styryl)-5*H*-4λ^4,5λ^4-dipyrrolo[1,2-*c*:2',1'-*f*][1,3,2]diazaborinine **5**.

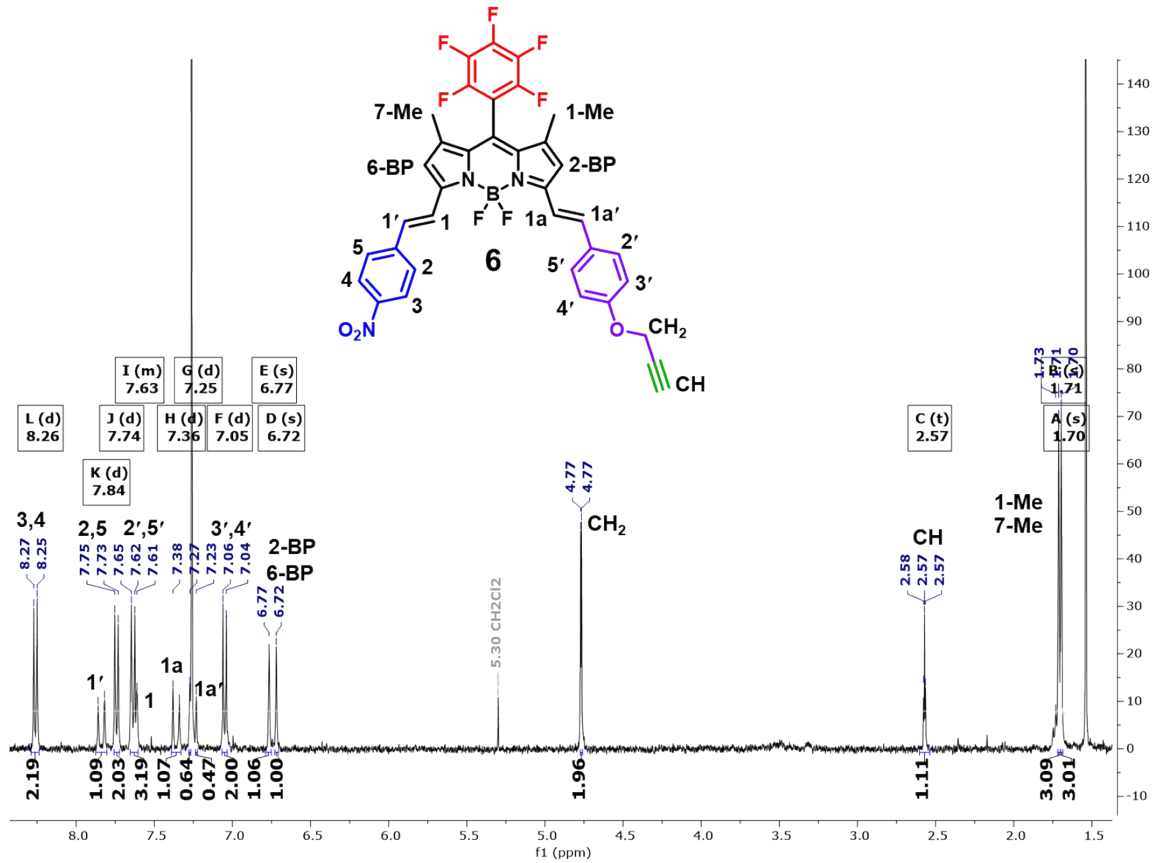

Figure S9. ^{1}H NMR-spectrum of **5,5-difluoro-1,9-dimethyl-3-((E)-4-nitrostyryl)-10-(perfluorophenyl)-7-((E)-4-(prop-2-yn-1-yloxy)styryl)-5*H*-4λ^4,5λ^4-dipyrrolo[1,2-*c*:2',1'-*f*][1,3,2]diazaborinine 6** in $CDCl_3$.

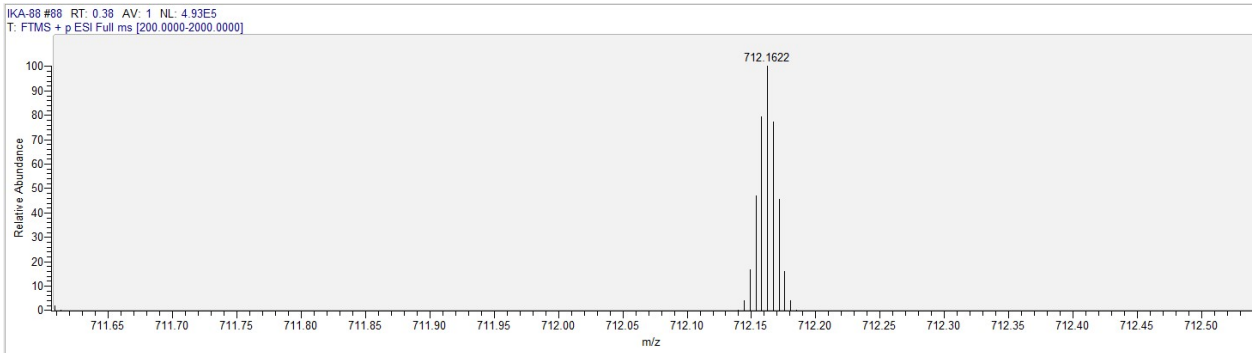

Figure S10. ESI-high resolution mass spectrum of **5,5-difluoro-1,9-dimethyl-3-((E)-4-nitrostyryl)-10-(perfluorophenyl)-7-((E)-4-(prop-2-yn-1-yloxy)styryl)-5*H*-4λ^4,5λ^4-dipyrrolo[1,2-*c*:2',1'-*f*][1,3,2]diazaborinine 6**.

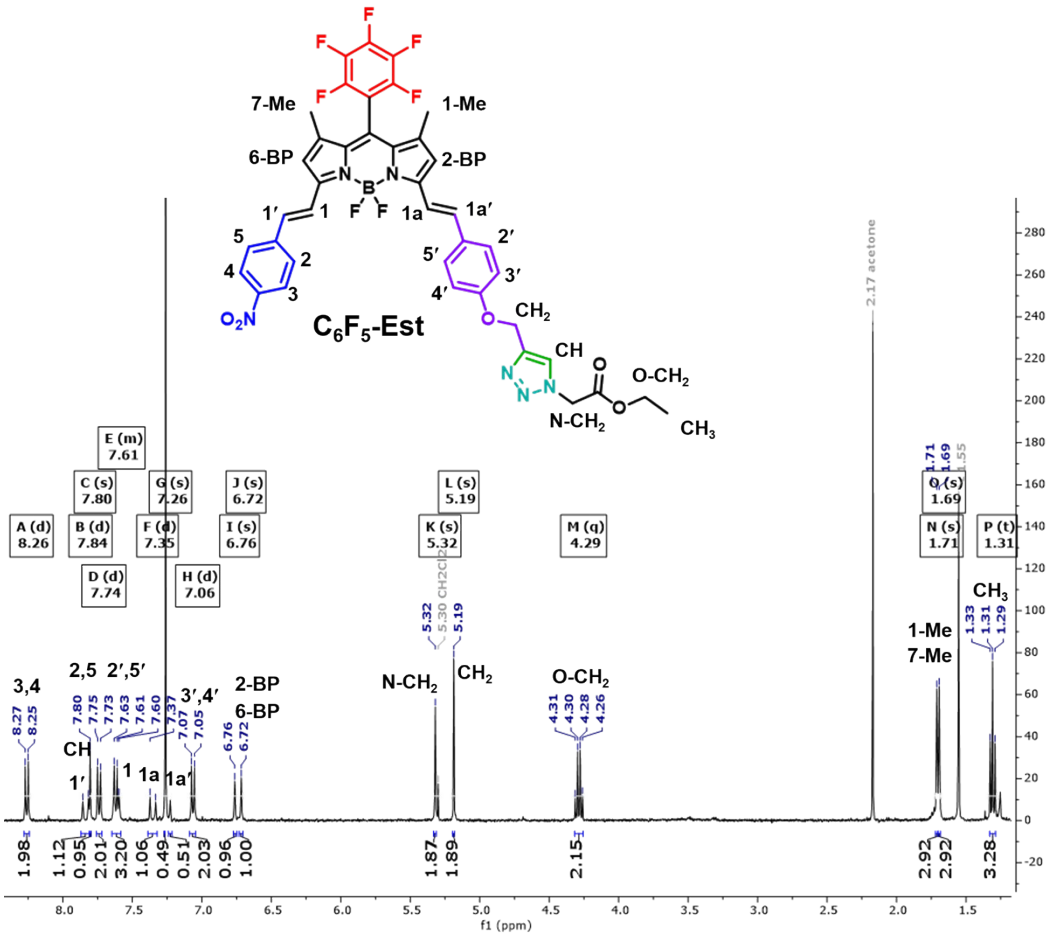

Figure S11. ^{1}H NMR-spectrum of **ethyl 2-(4-((4-((E)-2-(5,5-difluoro-1,9-dimethyl-7-((E)-4-nitrostyryl)-10-(perfluorophenyl)- 5*H*-4λ^{4},5λ^{4}-dipyrrolo[1,2-*c*:2',1'-*f*][1,3,2]diazaborinin-3-yl)vinyl)phenoxy)methyl)-1H-1,2,3-triazol-1-yl)acetate C_6F_5-Est** in $CDCl_3$.

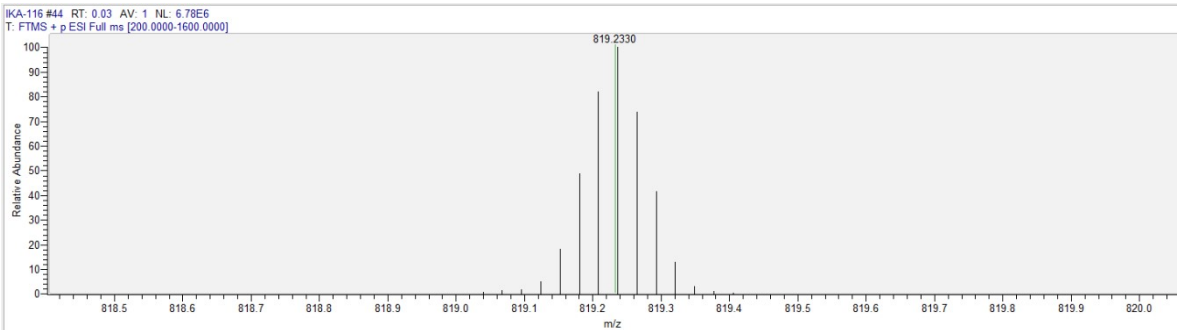

Figure S12. ESI-high resolution mass spectrum of **C_6F_5-Est**.

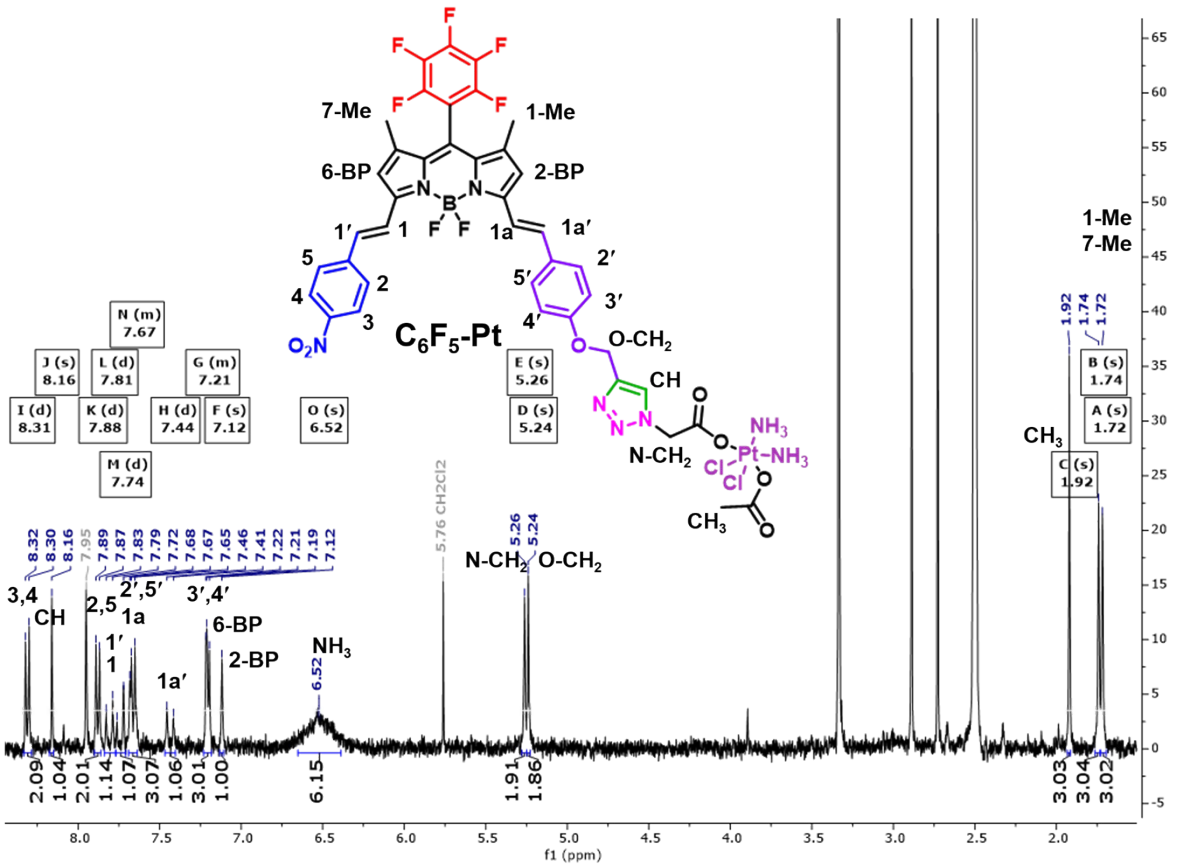

Figure S13. ^{1}H NMR-spectrum of **C_6F_5-Pt** in DMSO-d_6.

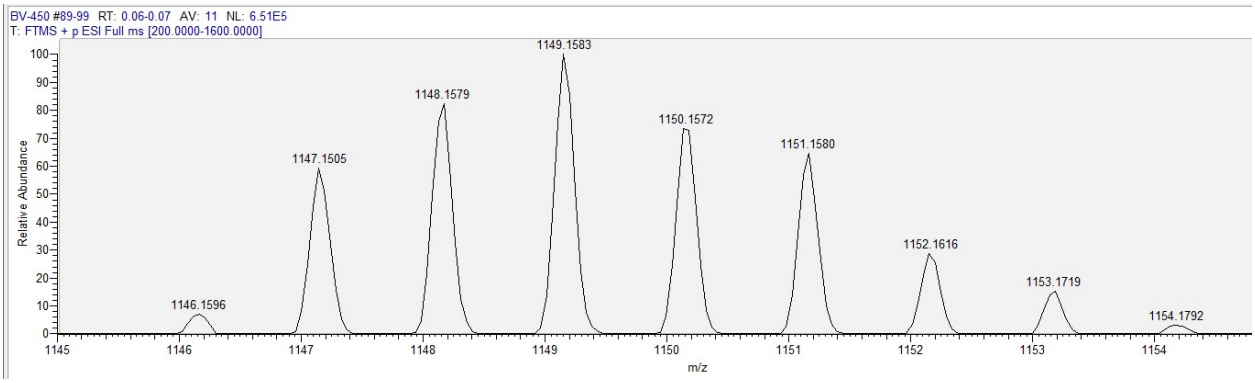

Figure S14. ESI-high resolution mass spectrum of **C_6F_5-Pt**.

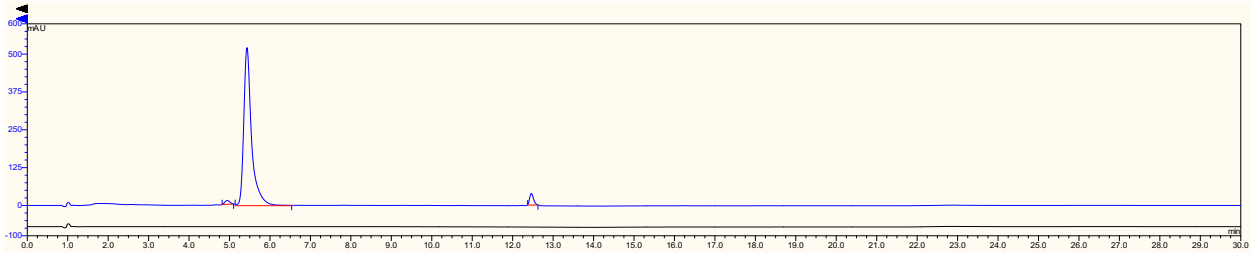

Figure S15. RP-HPLC analysis of **C_6F_5-Pt**. UV-VIS detector was set at 650 nm. Main peak area: 95.04%.

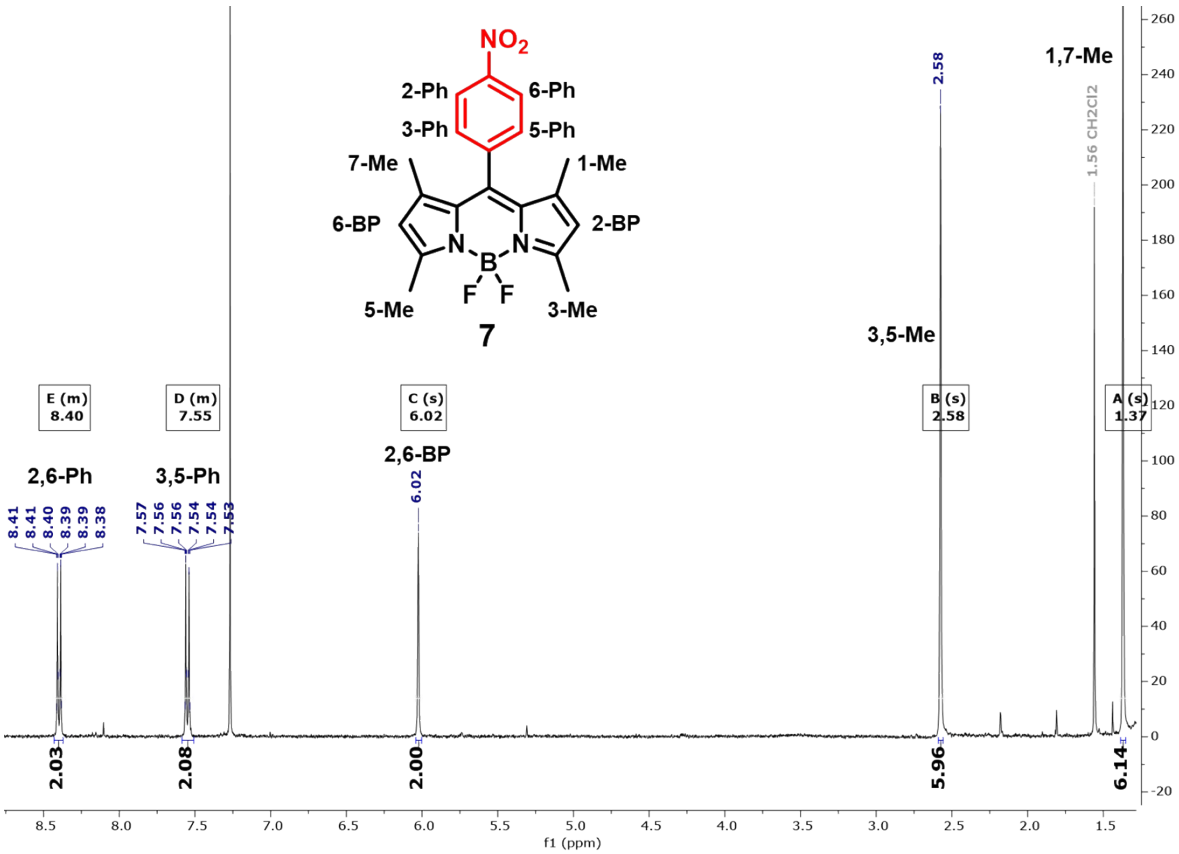

Figure S16. ^{1}H NMR-spectrum of **5,5-difluoro-1,3,7,9-tetramethyl-10-(4-nitrophenyl)-5*H*-4λ^{4},5λ^{4}-dipyrrolo[1,2-*c*:2',1'-*f*][1,3,2]diazaborinine 7** in $CDCl_3$.

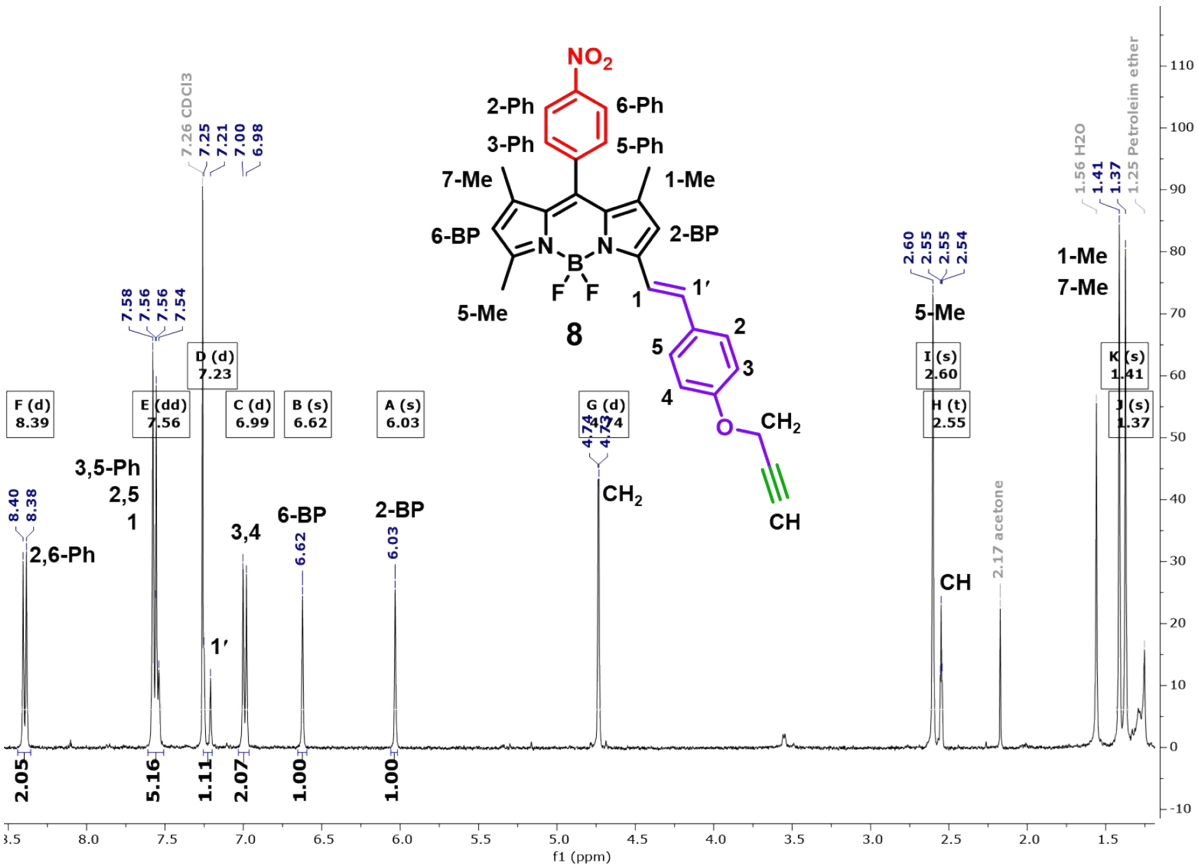

Figure S17. ^{1}H NMR-spectrum of **(*E*)-5,5-difluoro-1,3,9-trimethyl-10-(4-nitrophenyl)-7-(4-(prop-2-yn-1-yloxy)styryl)-5*H*-4λ^{4},5λ^{4}-dipyrrolo[1,2-*c*:2',1'-*f*][1,3,2]diazaborinine 8** in $CDCl_3$.

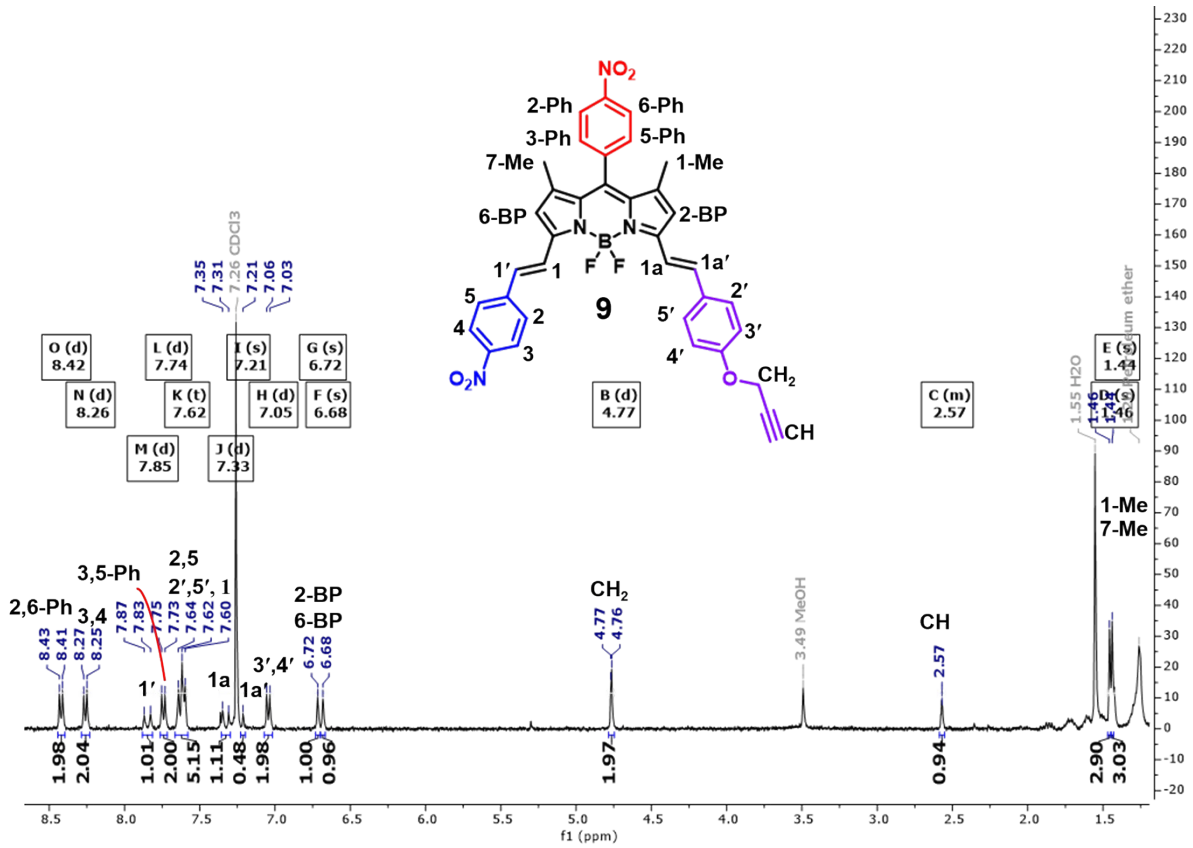

Figure S18. ^{1}H NMR-spectrum of **5,5-difluoro-1,9-dimethyl-10-(4-nitrophenyl)-3-((*E*)-4-nitrostyryl)-7-((E)-4-(prop-2-yn-1-yloxy)styryl)-5*H*-4λ^{4},5λ^{4}-dipyrrolo[1,2-*c*:2',1'-*f*][1,3,2]diazaborinine 9** in $CDCl_3$.

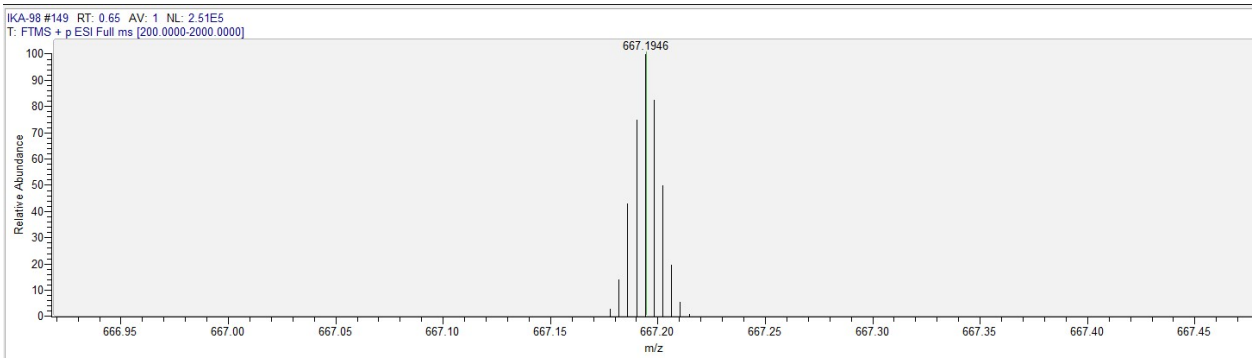

Figure S19. ESI-high resolution mass spectrum of **5,5-difluoro-1,9-dimethyl-10-(4-nitrophenyl)-3-((*E*)-4-nitrostyryl)-7-((E)-4-(prop-2-yn-1-yloxy)styryl)-5*H*-4λ^{4},5λ^{4}-dipyrrolo[1,2-*c*:2',1'-*f*][1,3,2]diazaborinine 9**.

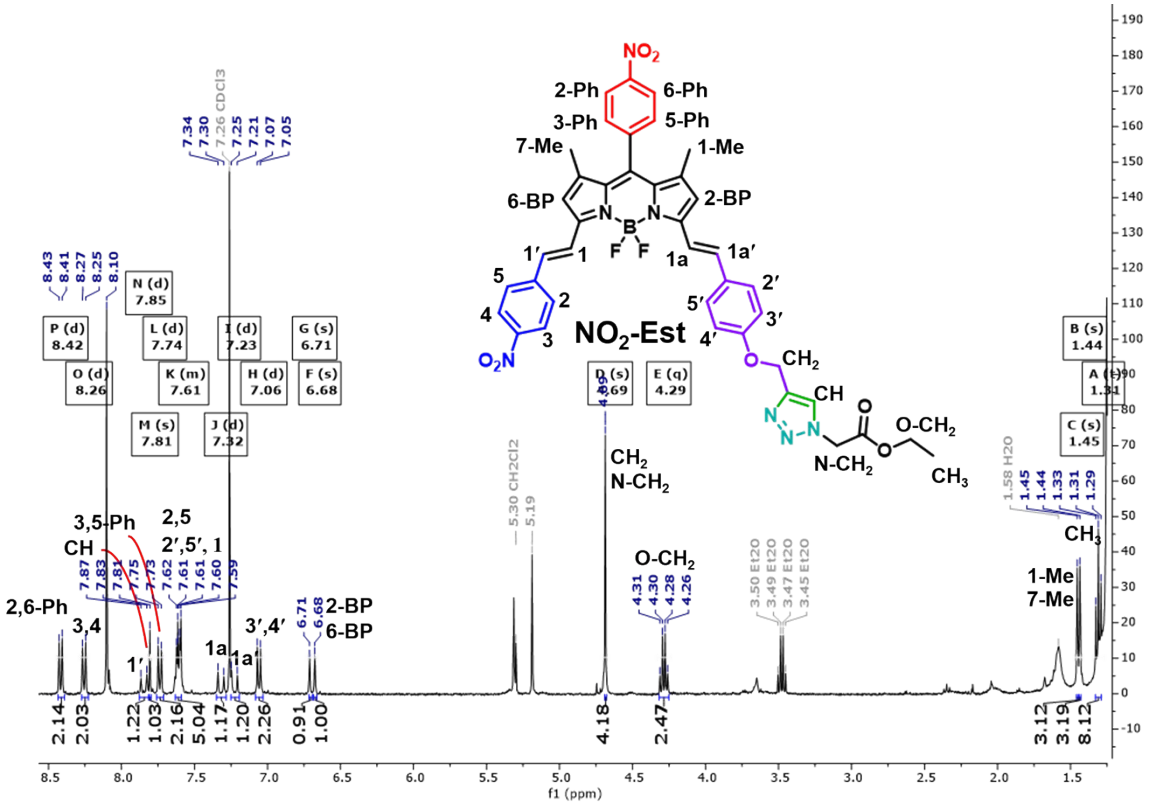

Figure S20. ^{1}H NMR-spectrum of **ethyl 2-(4-((4-((E)-2-(5,5-difluoro-1,9-dimethyl-10-(4-nitrophenyl)-7-((*E*)-4-nitrostyryl)- 5*H*-4λ^{4},5λ^{4}-dipyrrolo[1,2-*c*:2',1'-*f*][1,3,2]diazaborinin-3-yl)vinyl)phenoxy)methyl)-1H-1,2,3-triazol-1-yl)acetate NO_2-Est** in $CDCl_3$.

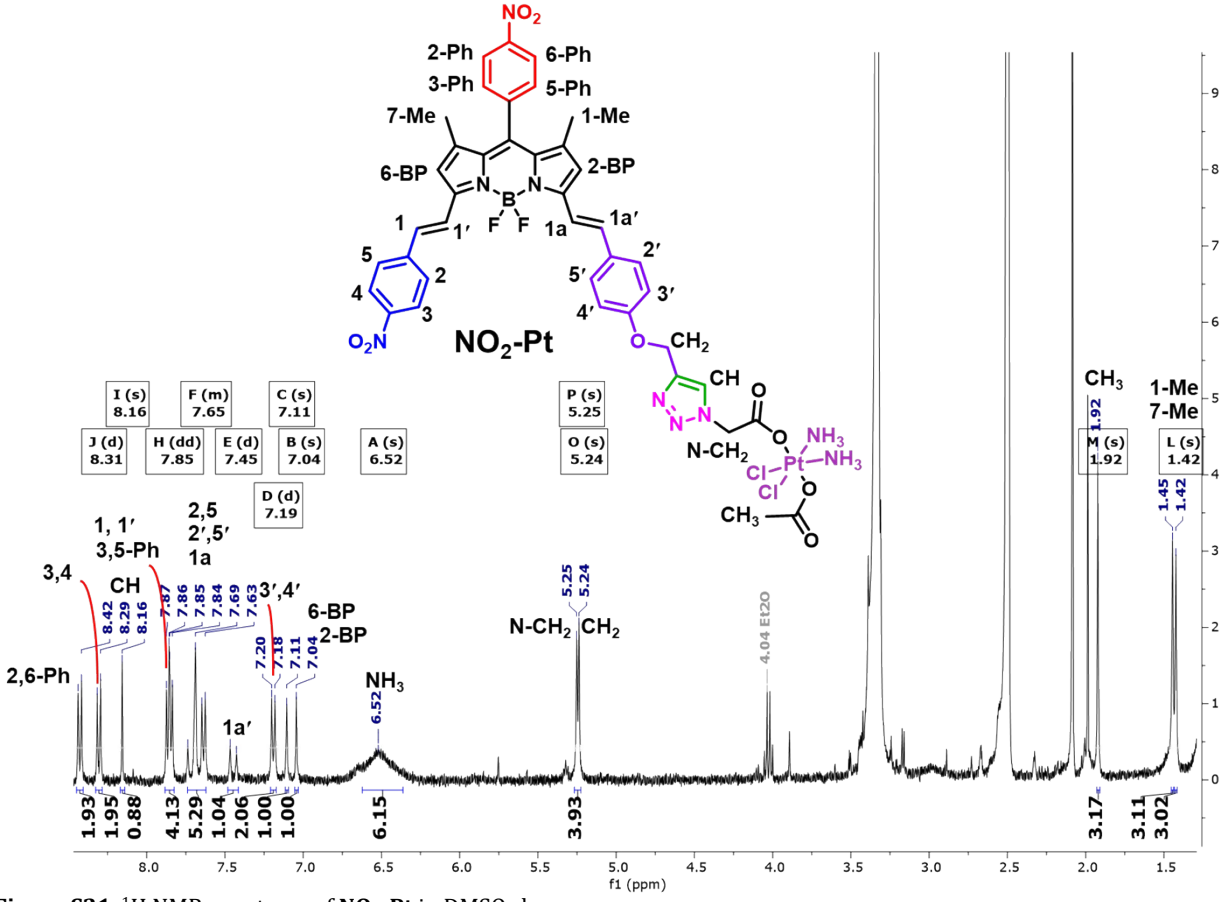

Figure S21. ^{1}H NMR-spectrum of **NO_2-Pt** in DMSO-d_6.

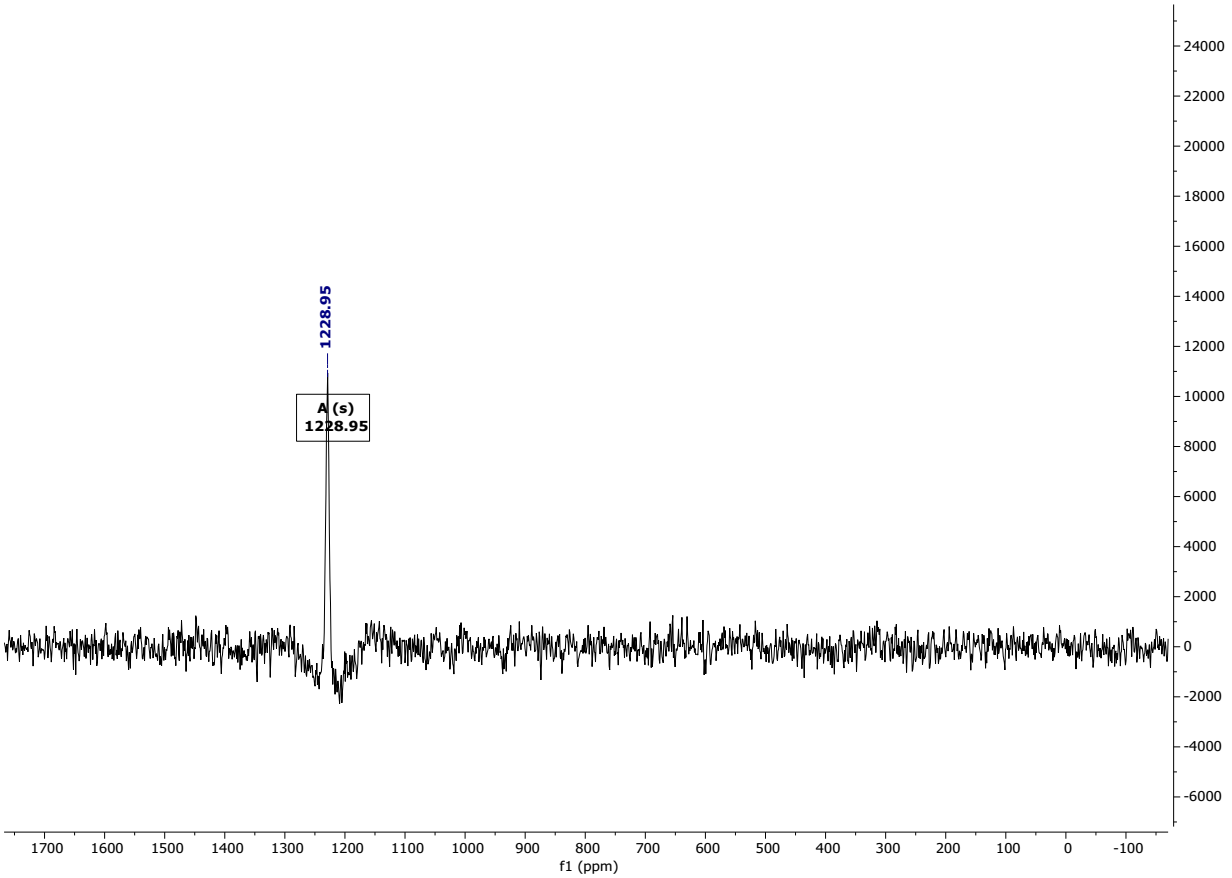

Figure S22. ^{195}Pt NMR-spectrum of **NO_2-Pt** in DMSO-d_6.

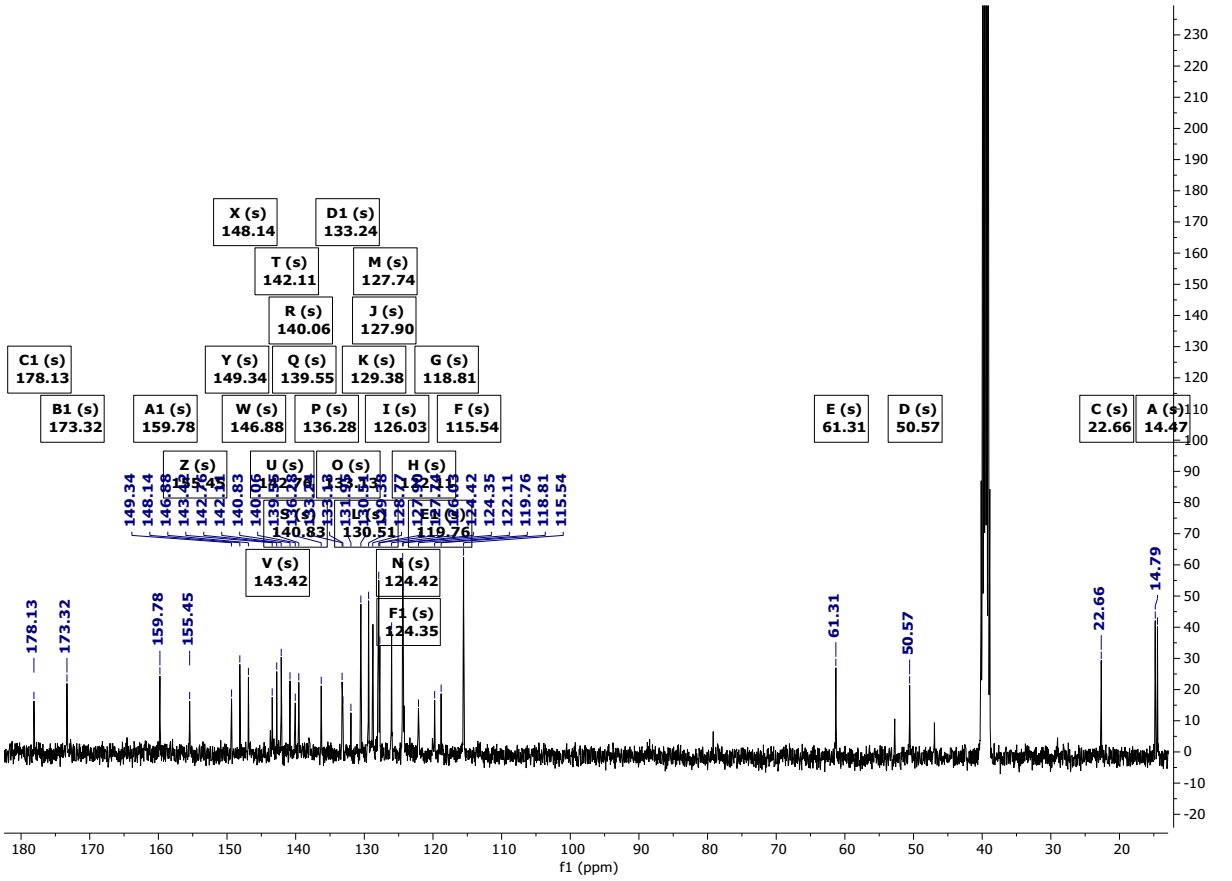

Figure S23. ^{13}C NMR-spectrum of **NO_2-Pt** in DMSO-d_6.

Figure S24. ESI-high resolution mass spectrum of **NO_2-Pt**, and RP-HPLC analysis of **NO_2-Pt**. UV-VIS detector was set at 650 nm. Main peak area: 95.55%

4. Photophysical properties of monomers& cisplatin release

Table S1. Quantum yield of singlet oxygen, quantum yield of fluorescence, absorption and emission wavelengths for **C_6F_5-Pt**, **C_6F_5-Est**, **NO_2-Pt**, **NO_2-Est** (CH_3CN, 10^{-5}M)

Compound	ΔΦ	Φ_{fl}	λ_{abs}	λ_{fl}
C_6F_5 -Est	~ 0.001	0.10	660	680
C_6F_5-Pt	~ 0.001	0.09	661	682
NO_2-Est	~ 0.001	0.04	644	669
NO_2-Pt	~ 0.001	0.04	646	672

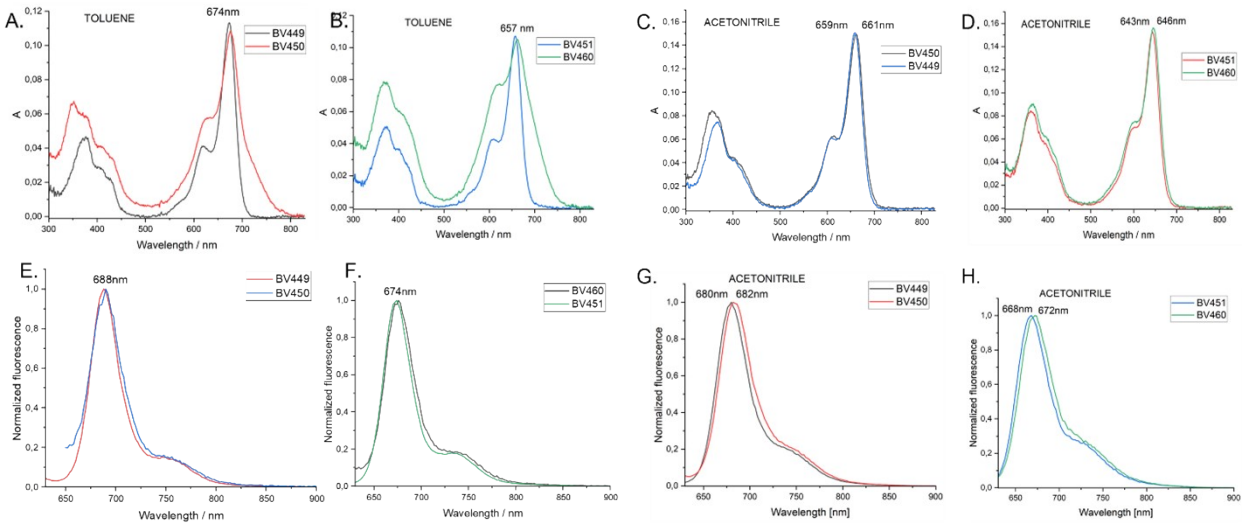

Figure S25. Absorption (A-D) and emission (E-H) spectra of **C_6F_5-Pt** (BV-450), **C_6F_5-Est** (BV-449), **NO_2-Pt** (BV-460), **NO_2-Est** (BV-451) in toluene and acetonitrile.

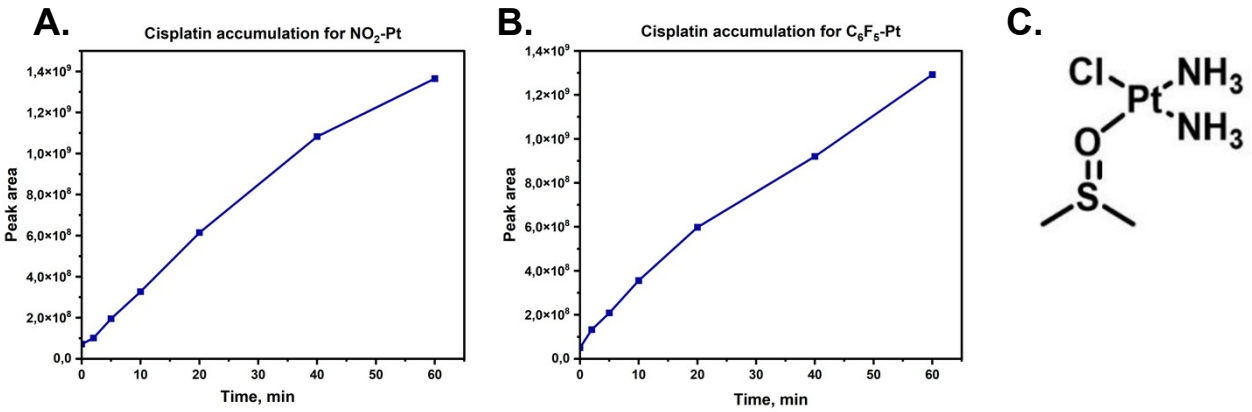

Figure S26. HPLC-MS monitoring of the accumulation of the cisplatin adduct $[Pt(NH_3)_2Cl(DMSO)]^+$ upon irradiation (660 nm, 13.5 mW/cm^2) of solutions of **NO_2-Pt** (**A**) and **C_6F_5-Pt** (**B**). **C**. Structure of cisplatin-DMSO adduct: one chloride ligand of cisplatin is replaced by DMSO.

5. Preparation and characterization of nanoparticles

5.1. Nanoparticles preparation

C_6F_5-Pt-F127-NPs, **C_6F_5-Est-F127-NPs, NO_2-Pt-NPs** and **NO_2-Est-NPs** were synthesized using the similar nanoprecipitation protocol.[5] Briefly, 40 mg of F127 was dissolved in 100 ml of pure distilled water under sonication for 15 minutes. Subsequently, 1000 µL of **BODIPY** solution (1 mg/ml in acetone) was added dropwise slowly to the F127 solution under vigorous stirring. After stirring for 1 hour, the solution was purified and concentrated by centrifugation (1800 rpm, 15 min) using centrifugal filters (Millipore Amicon Ultra-15, MWCO 30 kDa) and washed three times with clean distilled water (1800 rpm, 15 min). The concentrated nanoparticle solution was then passed through a 0.22 µm Millex-HV syringe filter to remove any aggregates. The resulting dark-colored solutions of **NPs** were then characterized via DLS and AFM. The concentration of the nanoparticles was determined spectrophotometrically. To assess the drug loading efficiency (DLE), the BODIPY content within the nanoparticles was quantified using a spectrophotometer (PerkinElmer Lambda 1050). This was done by applying previously obtained calibration curves for **BODIPY** in the concentration range of 0.005–0.0005 mg/ml, prepared in an aqueous solution of F127 (0.1 mg/ml).

C_6F_5-Pt-TF-NPs were prepared by thin-film hydration of BODIPY and F127.[2] Briefly, 1 mg of **C_6F_5-Pt** and 28 mg of F127 were dissolved by sonication in 6.3 mL of THF. The solvent was slowly removed under reduced pressure. The resulting residue was diluted with 15 mL of distilled water and sonicated in a water bath for 5 minutes. NPs solution was purified and concentrated by centrifugal ultrafiltration (1800 rpm, 15 min) using centrifugal filters (Millipore Amicon Ultra-15, MWCO 30 kDa) and washed four times with clean distilled water (1800 rpm, 15 min). The resulting dark-green nanoparticle suspension was passed through a 0.45 µm Millex-HV syringe filter to remove aggregates. The obtained nanoparticles were characterized via DLS.

An optimized nanoprecipitation protocol was employed for the preparation of **C_6F_5-Pt-DSPE-NPs** and **C_6F_5-Est-DSPE-NPs**. Briefly, 1000 µL of BODIPY solution (0.2 mg/mL in acetone) was mixed with 1000 µL of an aqueous DSPE-PEG_{2000}-OMe solution (1.8 mg/mL). The resulting mixture was subjected to sonication in a water bath maintained at 50 °C. Subsequently, 2.1 mL of ice-cooled pure distilled water (6 °C) was added dropwise over 10 seconds under continuous sonication. The mixture was further sonicated for 1.5 minutes. Thereafter, an additional 10 mL of distilled water (6 °C) was introduced over 40 seconds, followed by extended sonication for 1 minute. Obtained nanoparticle solutions were purified using centrifugal filters (Millipore Amicon Ultra-15, MWCO 30 kDa) to gradually remove residual acetone (1300 rpm, 6 °C, 20 min), and then washed three times with pure distilled water (1300 rpm, 15 °C, 20 min). To eliminate large aggregates, the nanoparticle suspension was passed through 0.45 µm Millex-HV syringe filters. The resulting dark-colored green solution of **C_6F_5-Est-DSPE-NPs** and light-colored blue solution **C_6F_5-Pt-DSPE-NPs** were then characterized via DLS and AFM. To assess the drug loading efficiency (DLE), the BODIPY content within the nanoparticles was quantified using a spectrophotometer (PerkinElmer Lambda 1050). This was done by applying previously obtained calibration curves for **C_6F_5-Est** and **C_6F_5-Pt** in the concentration range of 0.005–0.0005 mg/ml, prepared in an acetone:water (1:3) solution of DSPE-PEG_{2000}-OMe (0.1 mg/ml).

DLE was determined using the equation (1).

$$DLE = \frac{Mass\ of\ BODIPY\ loaded\ into\ the\ nanoparticles\ (mg)}{Initial\ mass\ of\ BODIPY\ (mg)} \times 100 \quad (1)$$

The measured DLE was 43.8% for **C_6F_5-Pt-F127-NPs,** 84.5% for **C_6F_5-Est-F127-NPs,** 56.0% for **NO_2-Pt-NPs,** 70.5% for **NO_2-Est-NPs,** 18.4% for **C_6F_5-Pt-DSPE-NPs** and 19.6% for **C_6F_5-Est-DSPE-NPs.**

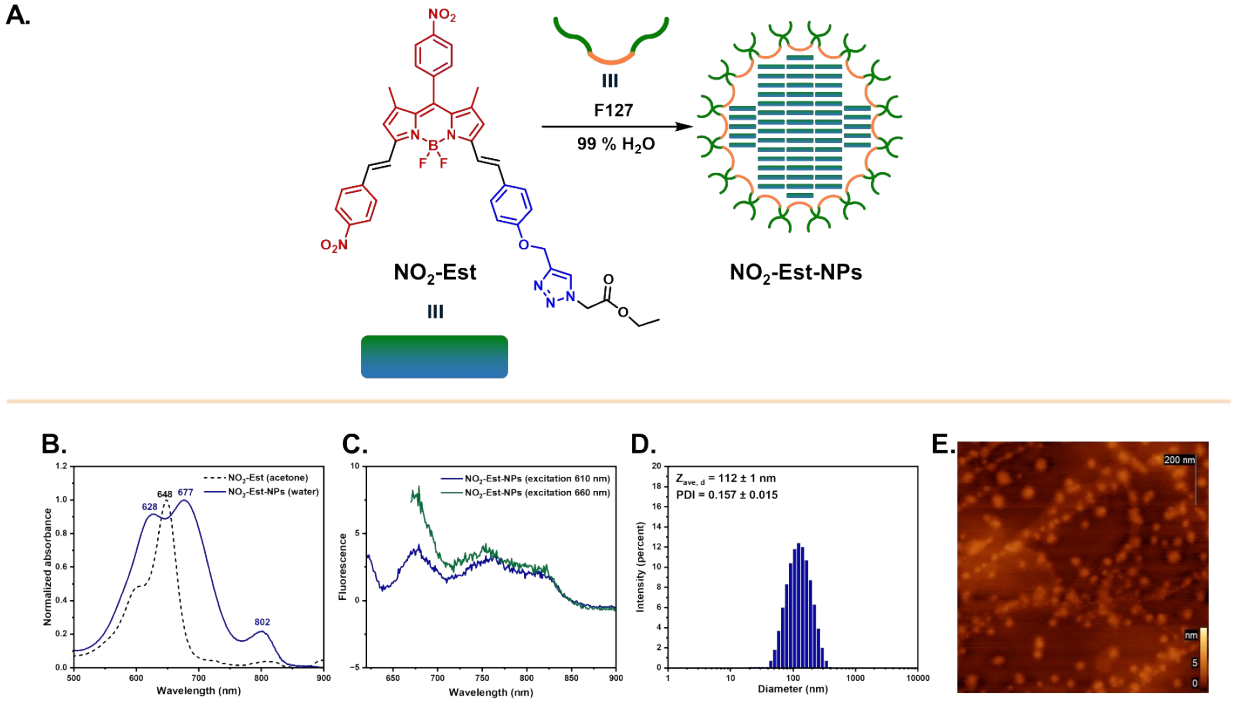

Figure S27. A. Synthesis scheme of **NO_2-Est-NPs**. B. Normalized absorption spectra of **NO_2-Est** and **NO_2-Est-NPs** in acetone and water respectively. C. Emission spectra (λ_{ex} = 610 nm and 660 nm) of **NO_2-Est-NPs** in water (C = 5 µM). D. Hydrodynamic size distribution of **NO_2-Est-NPs** obtained via DLS. E. AFM image of **NO_2-Est-NPs**. Scale bar: 200 nm

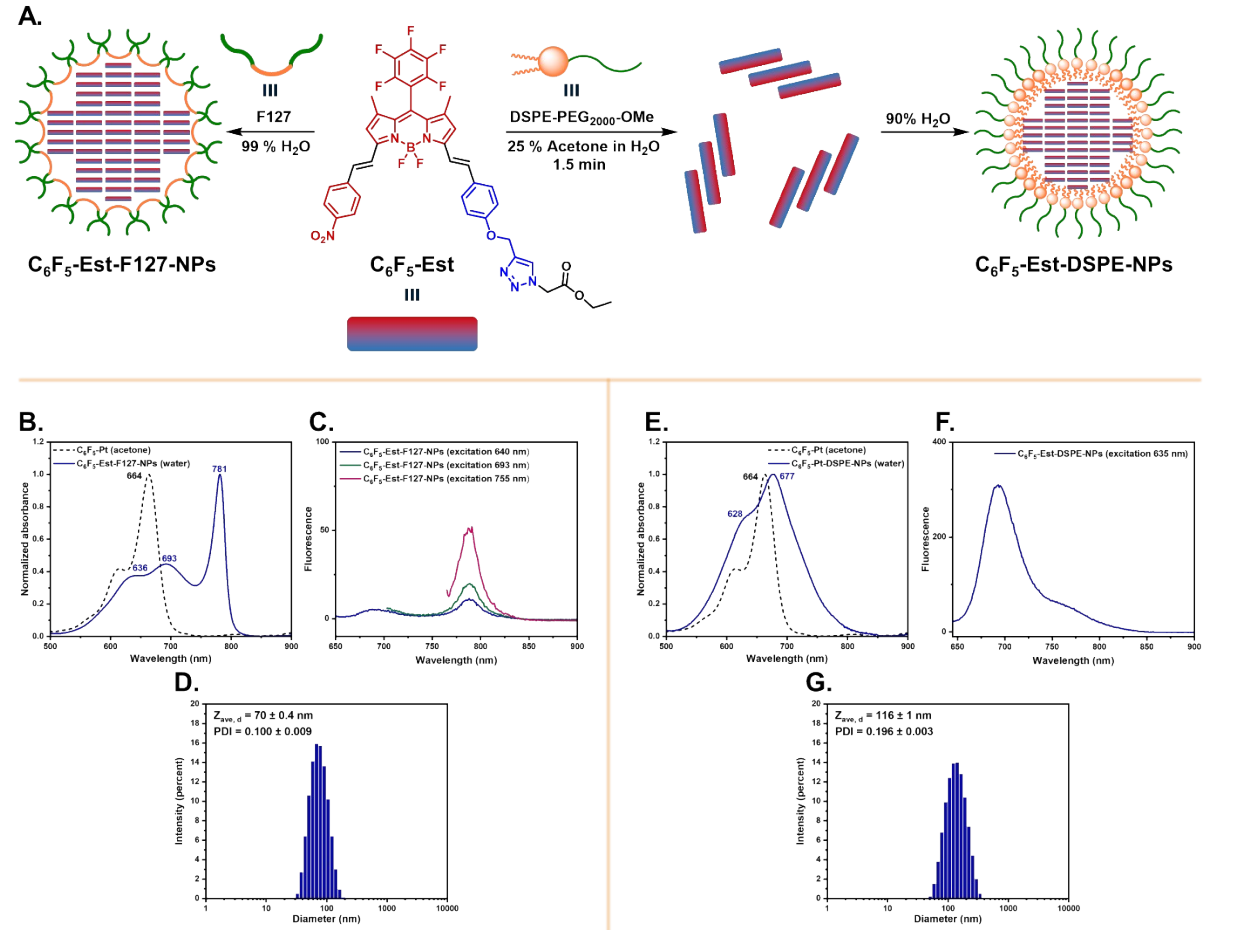

Figure S28. A. Synthesis scheme of **C_6F_5-Est-F127-NPs** and **C_6F_5-Est-DSPE-NPs**. B. Normalized absorption spectra of **C_6F_5-Est** and **C_6F_5-Est-F127-NPs** in acetone and water, respectively. C. Emission spectra (λ_{ex} = 640 nm, 693 nm and 755 nm) of **C_6F_5-Est-F127-NPs** in water (C = 5 μM). D. Hydrodynamic size distribution of **C_6F_5-Est-F127-NPs** obtained via DLS. E. Normalized absorption spectra of **C_6F_5-Est** and **C_6F_5-Est-F127-NPs** in acetone and water, respectively. F. Emission spectra (λ_{ex} = 635 nm) of **C_6F_5-Est-DSPE-NPs** in water (C = 2 μM). G. Hydrodynamic size distribution of **C_6F_5-Est-DSPE-NPs** obtained via DLS.

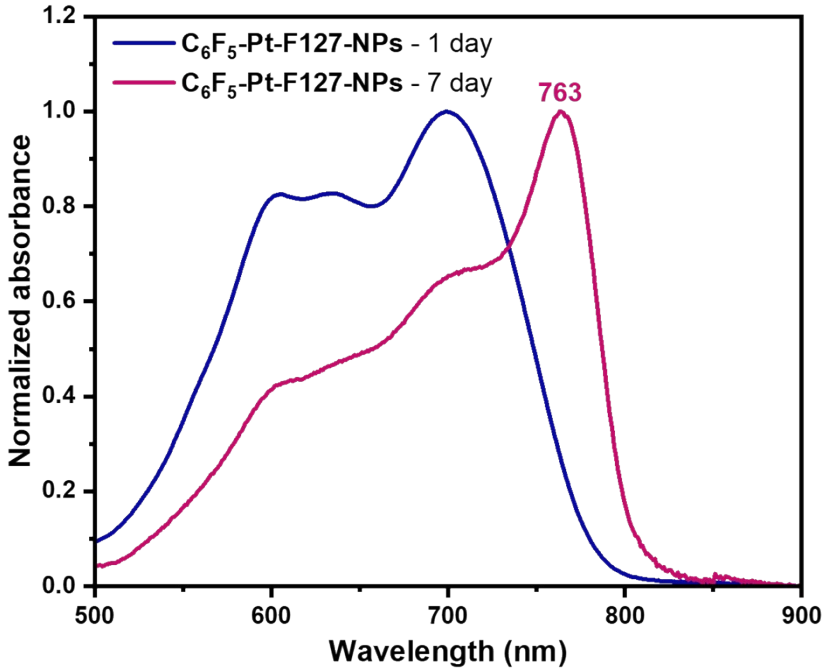

Figure S29. Normalized absorption spectra of **C_6F_5-Pt-F127-NPs** 1 (blue) and 7 days (pink) after synthesis.

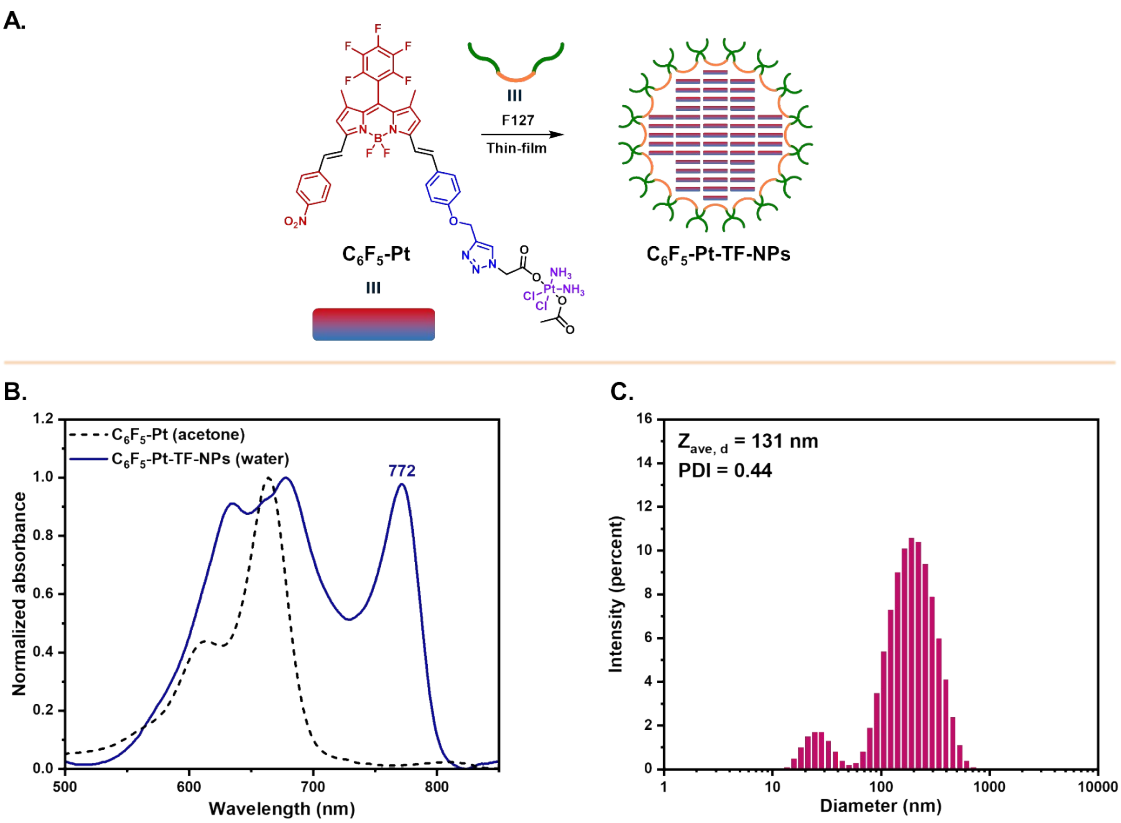

Figure S30. A. Synthesis scheme of **C_6F_5-Pt-TF-NPs**. B. Normalized absorption spectra of **C_6F_5-Pt** and **C_6F_5-Pt-TF-NPs** in acetone and water, respectively. C. Hydrodynamic size distribution of **C_6F_5-Pt-TF-NPs** obtained via DLS.

5.2. AFM characterization of nanoparticles

20 µl of each sample solutions were placed on a freshly cleaved highly oriented pyrolytic graphite (ZYH grade, NT-MDT SI, Russia), incubated for 30 min, rinsed with 1 ml of ultrapure water, and dried an argon flow. AFM images were processed in Femtoscan software (Advanced Technologies Center, Russia).[6] For the statistical analysis NPs were traced from the images by circular segments using the special tool in the software. The selected contours were converted into sequences of two-dimensional coordinates and the obtained data were presented as NPs diameters in the form of histograms with bin size 5 or 10.

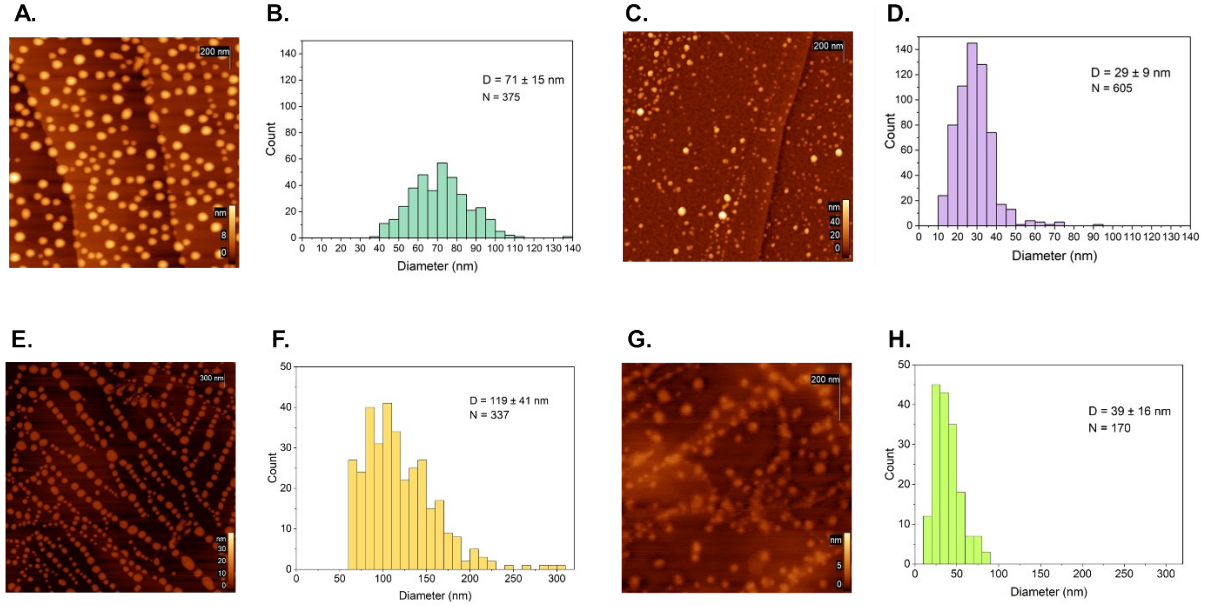

Figure S31. (A) AFM image of **C_6F_5-Pt-F127-NPs**. Scale bar: 200 nm. (B) Size distribution histogram via AFM of **C_6F_5-Pt-F127-NPs.** Bin size: 5 (C) AFM image of **NO_2-Pt-NPs**. Scale bar: 200 nm. (D) Size distribution histogram via AFM of **NO2-Pt-F127-NPs.** Bin size: 5 (E) AFM image of **C_6F_5-Pt-DSPE-NPs**. Scale bar: 300 nm. (F) Size distribution histogram via AFM

of **C_6F_5-Pt-DSPE-NPs.** Bin size: 10 (G) AFM image of **NO_2-Est-NPs**. Scale bar: 200 nm. (H) Size distribution histogram via AFM of **NO_2-Est-NPs.** Bin size: 10

5.3. Zeta-potential of nanoparticles

For the zeta-potential measurements were used aqueous solution of **BODIPY-NPs** (50 μM) 24 hours after their synthesis. Measurements were performed in triplicate. The measured zeta-potential was -16.0 ± 1.5 mV for **C_6F_5-Pt-F127-NPs**, -38.0 ± 2.8 mV for **C_6F_5-Pt-DSPE-NPs**, -28.3 ± 0.7 mV for **C_6F_5-Est-F127-NPs**, -21.0 ± 0.3 mV for **C_6F_5-Est-DSPE-NPs**, -20.4 ± 0.5 mV for **NO_2-Pt-NPs** and -32.1 ± 1.2 mV for **NO_2-Est-NPs**.

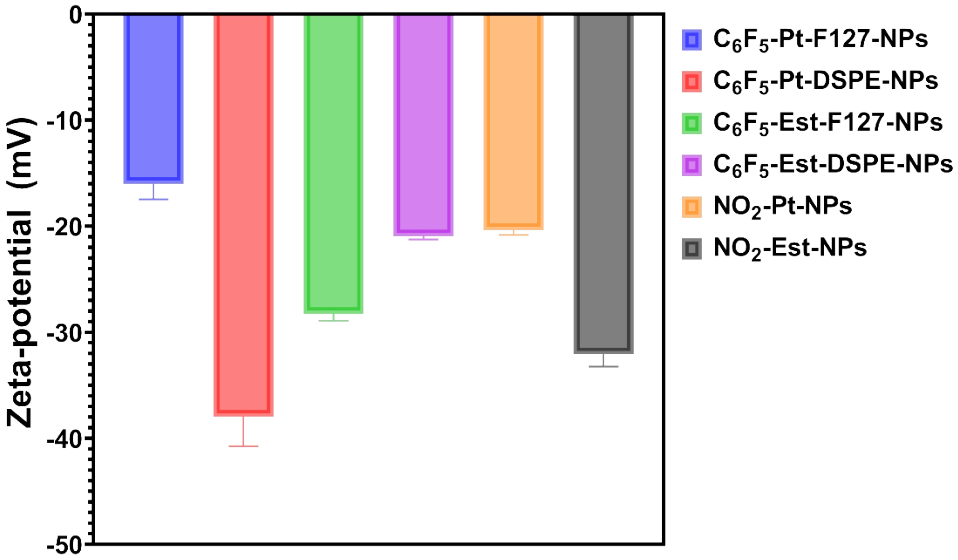

Figure S32. Zeta potential of obtained **BODIPY-NPs** detected by DLS.

5.4. Nanoparticles stability assay

Aqueous solutions of **BODIPY-NPs** (50 μM) were placed in sealed disposable cuvettes for DLS measurements and incubated at room temperature. At predetermined time intervals the hydrodynamic size of nanoparticles was measured by DLS. Measurements were performed in triplicate.

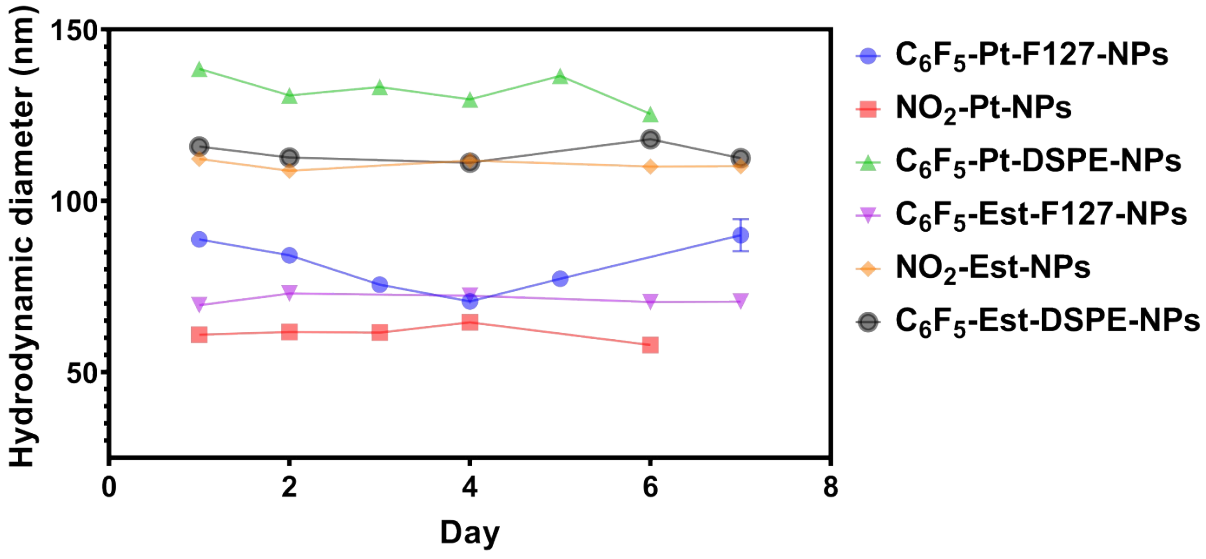

Figure S33. $Z_{average}$ hydrodynamic diameters of obtained **BODIPY-NPs** in water for 7 or 6 days determined by DLS.

5.5. ROS detection using H_2DCF-DA

ROS detection. 2',7'-dichlorodihydrofluorescein diacetate (H_2DCF-DA) was used as a chemical quencher for the detection of total ROS in solution according to generally accepted protocols with slight modifications.[7–9] The non-fluorescent 2',7'-dichlorodihydrofluorescein H_2DCF was prepared from H_2DCF-DA by alkaline hydrolysis. An aliquot of H_2DCF-DA (256 μL, 6269 μM) in methanol was adjusted to 4 mL with aqueous NaOH solution (1 mM) and left for 30 min at 10°C in the dark. The reaction mixture was then diluted to 40 mL with 10 mM PBS and thoroughly mixed. This resulted in a solution of H_2DCF

in 10 mM PBS with a concentration of 40 μM. This solution was used to prepare mixtures of **NPs** and H_2DCF (40 μM). These solutions (2 mL) were irradiated at 671 nm with vigorous stirring (2000 rpm) and thermostated at 25°C in cuvettes. The UV-Vis spectra of the solutions were recorded every 10 s during irradiation. Increase in optical density at 504 nm was observed, indicating accumulation of 2',7'-dichlorofluorescein (DCF), the product of the reaction of H_2DCF with ROS.

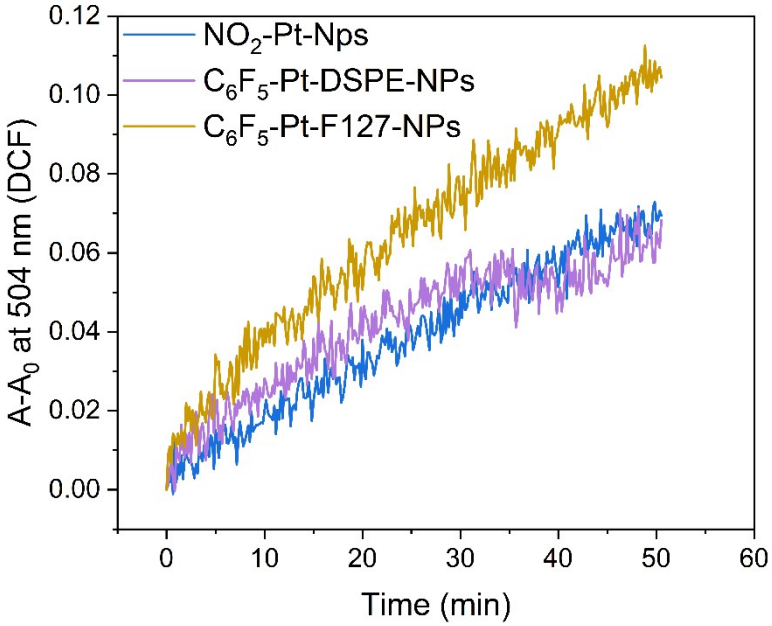

Figure S34. Changes in the UV-Vis spectra of solutions of H_2DCF (40 μM) and **BODIPY-NPs** in PBS under irradiation at 671 nm.

5.6. Photothermal conversion efficiency (PCE) of NPs.

The photothermal conversion efficiency (PCE) of **BODIPY-NPs** was calculated using previously published method.[10] To evaluate photoconversion ability, 100 μL solutions of **BODIPY-NPs** (100 μM) were irradiated with 745 nm or 660 nm LED at a power density of 120 mW/cm^2 and 450 mW/cm^2, respectively, and then the solution was allowed to cool to room temperature. The temperature was monitored throughout the entire heating and cooling cycle. The PCE was calculated using the Equation (2):

$$\eta = \frac{hA(T_{max} - T_{surr}) - Q_{DIS}}{I(1 - 10^{-A})} \quad (2)$$

where h represents the heat transfer coefficient, A is the surface area of the container, T_{max} is the steady-state temperature (the maximum temperature reached during the heating cycle), T_{surr} is temperature of the environment, Q_{Dis} is the heat dissipation property of the solvent and the container (see Equation(6)), I is the LED irradiation power density (W/cm2) and A is the average absorbance of the sample at FWHM of LED emission. hA coefficient could be calculated from the Equation (3):

$$\tau_S = \frac{m_D C_D}{hA} \quad (3)$$

where m_D is the mass of the solution (0.1 g) and cD is the heat capacity of H_2O (4.2 J/g). The τ_s parameter, which is the sample system time constant, could be calculated from the Equations (4) and (5):

$$t = -\tau_S ln\Theta \quad (4)$$

$$\Theta = \frac{T_{RT} - T_{surr}}{T_{max} - T_{surr}} \quad (5)$$

where Θ is the dimensionless driving force, T_{RT} is the real-time temperature at time point t of the cooling period. Thus, τ_s could be obtained from the linear fitting of -lnΘ and time t of the cooling period of the irradiated solution. The heat dissipation Q_{Dis} could be calculated from Equation (6):

$$Q_{DIS} = \frac{m_D C_D (T_{\max(water)} - T_{surr(water)})}{\tau_{S(water)}} \quad (6)$$

where $T_{max(water)}$ is the is the steady-state temperature of the solvent heating and cooling cycle and $\tau_{s(water)}$ is the system time constant of the solvent heating and cooling cycle. According to the obtained data and following the equations (2)-(6)

the photothermal conversion efficiency of **C_6F_5-Pt-F127-NPs, NO_2-Pt-NPs** and **NO_2-Est-NPs** was determined to be 31.6 %, 31.2 % and 32.7 % respectively.

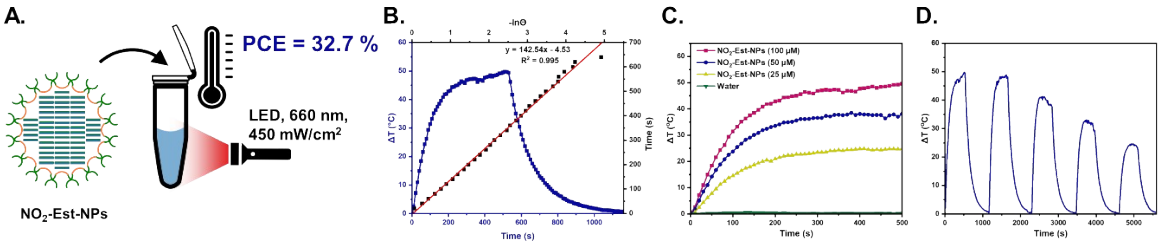

Figure S35. A. General scheme of photothermal properties evaluation of **NO_2-Est-NPs**. B. Temperature elevation and linear fitting of −lnΘ and time of the cooling curve of 100 μM **NO_2-Est-NPs** solution under 660 nm LED (450 mW/cm^2). C. Temperature elevation curves of various **NO_2-Est-NPs** solutions (25–100 μM). D. Temperature elevation curves of 5 heating–cooling cycles of 100 mM **NO_2-Est-NPs** solution.

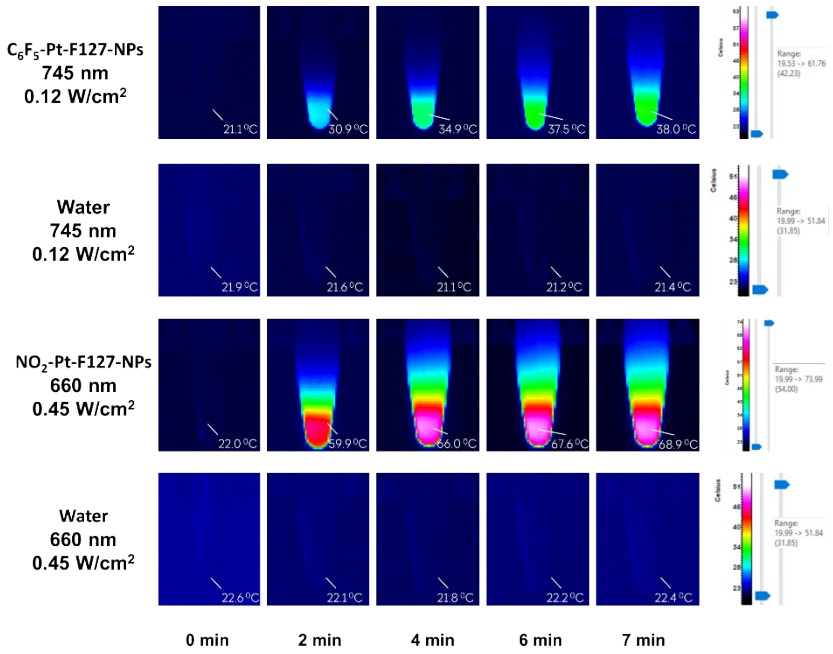

Figure S36. Infrared thermal images of 100 μM NPs solutions and water under 745 nm (0.12 W/cm^2) and 650 nm (0.45 W/cm^2).

5.7. Light-induced platinum release from C_6F_5-Pt-F127-NPs and NO_2-Pt-NPs

Release studies protocol

The solutions of **C_6F_5-Pt-F127-NPs** and **NO_2-Pt-NPs** was washed three times with pure distilled water using centrifugal filters (Millipore Amicon Ultra-0.5, MWCO 30 kDa) at 9000 rpm for 12 minutes to remove any low-molecular weight Pt impurities prior to the start of the experiment. The solution of **CF_3-Pt-NPs** was adjusted with pure distilled water to concentrations 6.5 mg/L of Pt and was irradiated with 650 nm LED (400 mW/cm^2) under constant stirring. A solution kept in the dark served as a control.

At predetermined time points, an aliquot of either the irradiated solution or the control solution was transferred to a centrifuge filter (Millipore Amicon Ultra-0.5, MWCO 30 kDa), diluted with pure distilled water, and centrifuged at 10 000 rpm for 10 minutes. This process was performed in triplicate for each time point. The platinum concentration in the filtrate and platinum concentration at the start of the experiment were subsequently determined by ICP-MS. Release was determined using Equation (7).

$$\%\ of\ released\ Pt = \frac{Concentration\ of\ Pt\ in\ filtrate}{Total\ concentration\ of\ Pt\ in\ the\ solution} \times 100 \quad (7)$$

5.8. Quantum-chemical calculations

Quantum-chemical calculations were performed in ORCA 6.0.1 package.[11,12] The analysis of computational results was performed using the Multiwfn 3.8(dev) package. [13]

C_6F_5-Pt monomer. Geometry optimization was performed using the composite electronic-structure method r2SCAN-3c [14] Implicit solvation was described with the solvation model based on density (SMD)[15] model using parameters for acetone. Single-point and linear-response TDDFT calculations on the optimized monomer geometries were performed with the range-separated CAM-B3LYP functional with relativistic full-electron basis sets (ZORA-def2-TZVP for light elements and SARC-ZORA-TZVP for Pt) within relativistic ZORA approximation.[16,17] Solvent effects were included via SMD (acetone). Excited states were obtained within the Tamm–Dancoff approximation (TDA), requesting 10 singlet roots; triplet states were not computed.

C_6F_5-Pt dimer. A representative **C_6F_5–Pt** dimer geometry was generated in vacuo using Docker (ORCA's module).[18] The lowest-energy docking pose (prior to any local optimization) was selected and subjected to a short pre-relaxation with r^2SCAN-3c in the presence of implicit solvent. Specifically, 100 geometry-optimization steps were performed with SMD parameters for water. Single-point and TDDFT calculations on the pre-relaxed dimer were performed with the range-separated CAM-B3LYP functional with relativistic full-electron basis sets (ZORA-def2-TZVP for light elements and SARC-ZORA-TZVP for Pt) within relativistic ZORA approximation. Solvation was described with SMD (water). TDDFT was performed within TDA, requesting 5 singlet roots; triplet states were not computed.

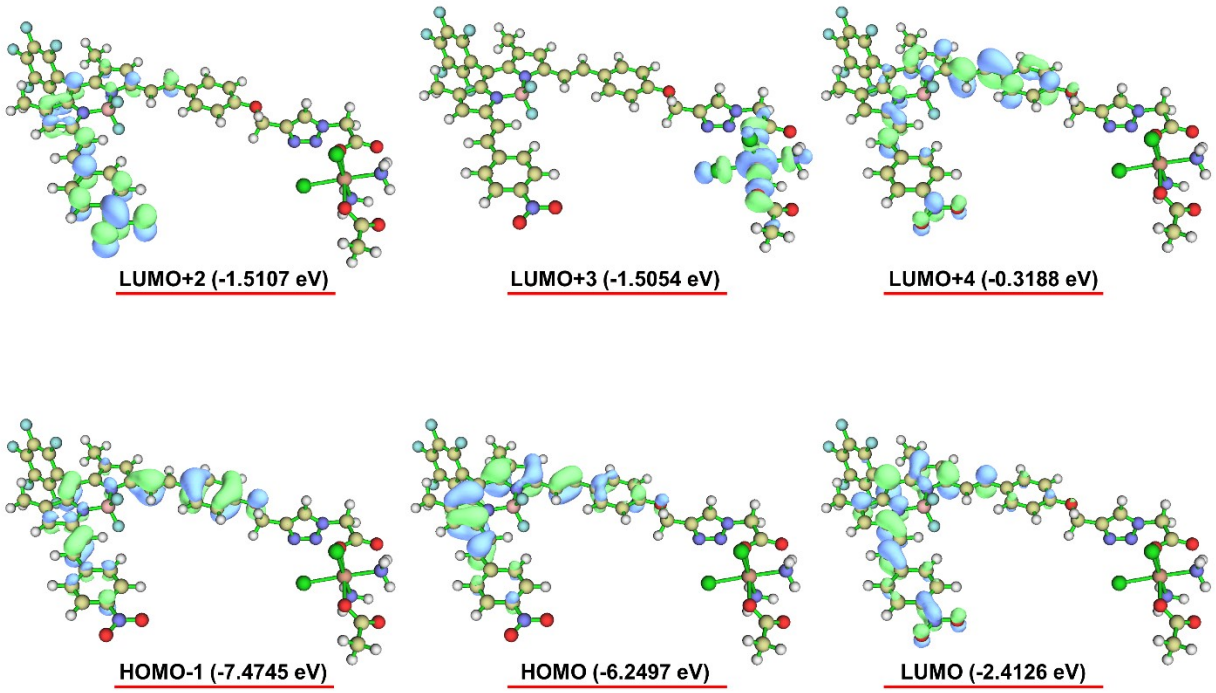

Figure S37. Molecular orbitals of **C_6F_5-Pt** involved in $S_0 \rightarrow S_1$ transition and lowest Pt-centered molecular orbital (LUMO+3) at an isosurface value of 0.035 a.u.

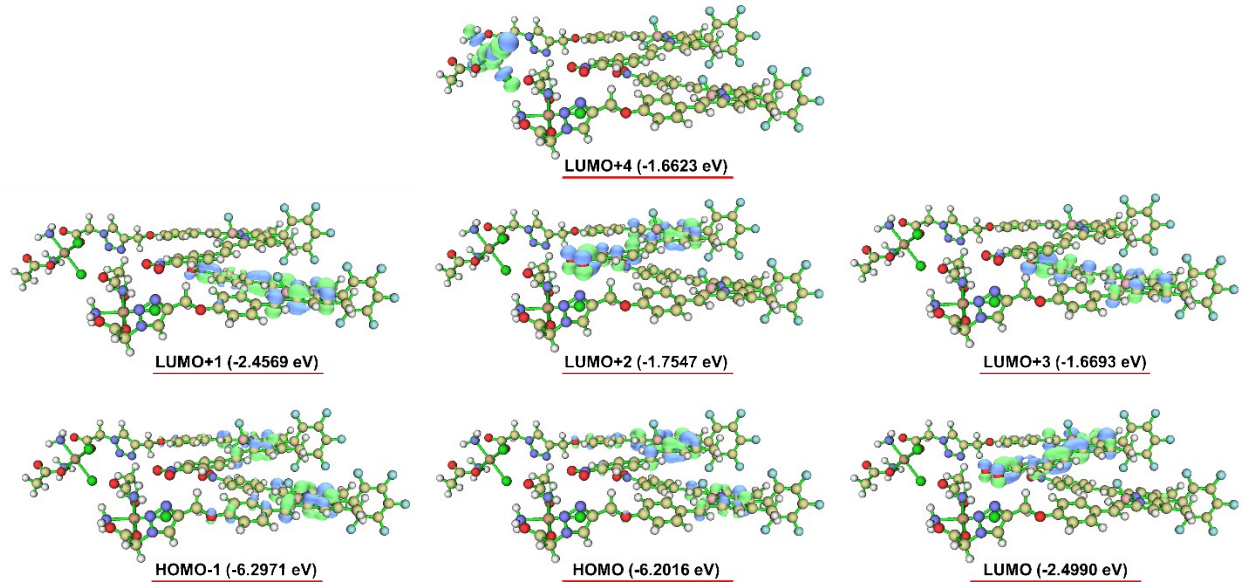

Figure S38. Molecular orbitals of **C_6F_5-Pt-dimer** involved in $S_0 \rightarrow S_{1\text{-}3}$ transitions and lowest Pt-centered molecular orbital (LUMO+4) at an isosurface value of 0.035 a.u.

Table S2. Calculated electronic excitations energies, oscillator strengths and the related wave functions.

	Excited state	Energy (eV)	λ (nm)	*f* (Oscillator strength)	MOs involved in the transitions
C_6F_5-Pt	S_1	2.08	595.6	1.44	H→L (93%), H→L+2 (1.0%), H-1→L+2 (1.1%), H-1→L+4 (1.3%).
C_6F_5-Pt dimer	S_1	1.99	622.7	0.09	H→L (25%), H-1→L (29%), H-1→L+1 (6.1%), H→L+1 (31%) H→L+2 (1.2%)
C_6F_5-Pt dimer	S_2	2.07	599.1	2.51	H→L (39%), H-1→L+1 (33%), H-1→L+3 (1.9%), H→L+1 (17%) H→L+2 (1.5%)
C_6F_5-Pt dimer	S_3	2.35	527.0	0.06	H→L (2.4%), H→L+1 (37%), H→L+3 (10%), H-1→L (4%) H-1→L+1 (41%) H-1→L+3 (3.6%)

Neutral C_6F_5-Pt (S0)

B	-0.92317728706723	-3.03716733098207	-0.07781772734588
N	-2.17222981689864	-3.94935679135754	-0.14359437320949
C	-3.47449975521060	-3.53561219494344	0.06939728922265
C	-3.75488880852913	-2.19047903987495	0.36650843599385
C	-2.73756697645448	-1.24718608768899	0.46642190272182
N	-1.41051896893280	-1.61228689935630	0.27652894434406
C	-0.62888290535088	-0.50260194609875	0.41377254363012
C	-1.47550026140804	0.60530553823273	0.70076531490768
C	-2.77815566076742	0.16699185338213	0.73691558819703
C	-4.33737063986364	-4.67136558595614	-0.06044963938572
C	-3.51942152588250	-5.74610357586621	-0.35521700713033
C	-2.18026713326528	-5.29271507792383	-0.40711243373078
F	-0.02945547533448	-3.50720210851711	0.90615991316219
F	-0.25919585680960	-3.03078465388699	-1.32185128779986
C	-5.16334294218261	-1.77202688002688	0.57021944091818
C	-5.71518158896714	-1.67821984177755	1.84188419566808
C	-7.03071522015834	-1.29047770386705	2.04304088931205

C	-7.82612919157472	-0.98447109168525	0.94754932632431
C	-7.30254032575908	-1.06874565107962	-0.33514860274374
C	-5.98453354663658	-1.46171337638355	-0.50706702903630
F	-9.09300329946923	-0.60863307925916	1.12783734794694
C	-3.96333073796168	1.02759708443842	1.01267998372738
C	-5.82096066693103	-4.74192771434818	0.08122523980248
C	-0.98415489618779	-6.02327501336385	-0.68006514149814
C	0.78769222427275	-0.53674343973869	0.27178983638756
C	1.56870771357770	0.57346694395710	0.37489719875865
C	-0.96168904260422	-7.35157384626035	-0.96135223508769
C	3.00241264541076	0.62978144370271	0.23679549647562
C	0.22204459884566	-8.13065093454414	-1.24779388938480
C	3.64140126231023	1.88524287577175	0.33192990556127
C	5.00727449774492	2.01172291845483	0.19064929989652
C	5.79204248866928	0.87466697749166	-0.05191499220940
C	5.18486079885204	-0.38828331896909	-0.13822019644874
C	3.81222630897405	-0.49837593120443	0.00371941197096
C	0.06780900256888	-9.50543318741316	-1.52464202629049
C	1.15579833011453	-10.31063292005859	-1.80373717663151
C	2.42718432751597	-9.74009563077823	-1.80925008643511
C	2.62065867383050	-8.38285307906942	-1.54235027479521
C	1.52645568362733	-7.58951331326337	-1.26504989724196
O	7.11908896038069	1.09845284010729	-0.18786416791025
N	3.58176191970944	-10.57858409499069	-2.09844878605042
O	4.69703372033885	-10.05382410536371	-2.10040341349466
O	3.39038159292775	-11.77447347330062	-2.32728998970198
C	7.97535172408789	-0.03551956988383	-0.48271812908065
C	9.34997381128639	0.47863736255360	-0.68946304060626
N	9.77580321505414	0.92623528582023	-1.90640804706697
N	11.01217591558041	1.32765655734561	-1.80330797453616
N	11.38823195554594	1.15611874029765	-0.52034853159399
C	10.38652350024116	0.61967649870166	0.20718869087605
C	12.76913954382852	1.38707567353437	-0.14493192192374
C	13.69426916607382	0.21597231501736	-0.49859963873525
O	14.89632760824342	0.42543083473701	-0.63560786848969
H	-1.14665354362701	1.62273296786062	0.86325324413372
H	-3.84799749721646	-6.76410575724787	-0.51594306272726
F	-4.96734044276344	-1.97257600940709	2.91439492450867
F	-7.53645466853606	-1.20616134429946	3.27767075907413
F	-8.06905904666664	-0.77124536776122	-1.38921893878416
F	-5.50086788670501	-1.53928949334500	-1.75448294264989
H	-3.64605382778726	2.07094089085686	1.09071784358143
H	-4.71723260664485	0.95664506539275	0.22150125205605
H	-4.45294194192426	0.75423051447977	1.95443230747476
H	-6.33309761613115	-4.18573143369961	-0.71230142580384
H	-6.14320450303366	-5.78483939839233	0.01860506220139
H	-6.16473447724125	-4.33486917013367	1.03789655784874
H	-0.05553007761998	-5.46113687276969	-0.65990790167731
H	1.24098578690615	-1.50196942930419	0.06778925465468
H	1.09020601850741	1.53209116516655	0.57169174743222
H	-1.89864149689421	-7.90546022056722	-0.98098402201890
H	3.03917780607227	2.77184250663752	0.51518517291472
H	5.49006760989769	2.98211809141275	0.25949945347939
H	5.77052346443221	-1.28325322609105	-0.31416453838740
H	3.36641584702159	-1.48604845938617	-0.06941428491844
H	-0.92872402114644	-9.93854042636013	-1.51697922982799
H	1.02765247408975	-11.36589397423529	-2.01426901824527
H	3.61963944113331	-7.96303984945146	-1.55315316723584
H	1.68863791604817	-6.53673512462042	-1.05783031410431
H	7.94877988078999	-0.74440642576426	0.35363635889244
H	7.62274552061760	-0.53287690874272	-1.39453911572031
H	10.48601119167330	0.38388905946965	1.25686805593188
H	13.13389752881232	2.28138325197602	-0.65633327168311
H	12.82359658254330	1.55039931039190	0.93657133181205
O	13.05753034709115	-0.91053420866812	-0.58844821080016
Pt	13.89550117677996	-2.67689301724231	-1.23078173749308
N	14.21662826008699	-1.79762712781146	-3.09273267764292
Cl	13.50687818878591	-3.61676865776526	0.89403979344859
Cl	11.72224525718620	-3.21136514389821	-2.00694052469602
H	15.18323550681857	-1.50236396324187	-3.22135773430828
H	13.98928671766707	-2.45998704902707	-3.83356592465719
H	13.60463635636776	-0.98804847184665	-3.19953123980370
O	14.50391332185410	-4.52114021811846	-1.86092170543641
C	15.57628652921763	-4.67193303935249	-2.60593699918493
C	15.79146467454768	-6.10869268036725	-3.01285434428834
H	15.61106543023629	-6.18403827661992	-4.09108233963241
H	15.12714047815583	-6.79709838007610	-2.48907473496832

H	16.83581965581910	-6.37626926556558	-2.82875294355658
O	16.33609073731571	-3.77304907980750	-2.96479070816711
N	15.82080283831211	-2.22913597584992	-0.58927335644068
H	15.88105324293322	-1.21017747698290	-0.47625243479850
H	16.01318281877615	-2.69384230364171	0.29730119285964
H	16.48161638803458	-2.55535285064653	-1.29878613285600

Neutral C_6F_5-Pt-dimer (S0)

B	-5.31599825545251	-1.51637495128604	0.92185838267416
N	-6.43006304923759	-2.58578812541783	0.86421026581129
C	-7.78650521333101	-2.32635283784741	0.79789796406998
C	-8.25186556258697	-1.00189458521707	0.72433491536923
C	-7.36925243363567	0.07379273404685	0.72402647203776
N	-6.00044423703850	-0.13549035683749	0.82361647320847
C	-5.36757838800954	1.07165743570595	0.77088388262376
C	-6.35429611990324	2.08648040798447	0.63097338942636
C	-7.59521171862030	1.49144026663326	0.60196043545583
C	-8.48599587126279	-3.57673789198761	0.81219351137389
C	-7.51716955433972	-4.56176736811066	0.86765218518230
C	-6.24628652486888	-3.94058315865653	0.90370106898789
F	-4.41339229414938	-1.69657256853205	-0.14621056654909
F	-4.60077786797885	-1.61899244366468	2.13426064123473
C	-9.70968373384487	-0.75316684079650	0.63284701210022
C	-10.38490462205037	-0.85163930238217	-0.57695315728253
C	-11.74835502313732	-0.62504700569479	-0.67461311552822
C	-12.46679892635280	-0.29424071931770	0.46567930635334
C	-11.81934397491829	-0.19052300588616	1.68879853011294
C	-10.45454249210052	-0.41948412534484	1.75692317989600
F	-13.77968216680602	-0.07383738472203	0.38593955665422
C	-8.89276249253055	2.21189930679756	0.47096277594344
C	-9.95589887364815	-3.83017856964111	0.78389523528759
C	-4.94916873670585	-4.52223026203616	1.00680834311748
C	-3.95157555677445	1.18366902456670	0.85443505867517
C	-3.27105734792799	2.34942714250269	0.68977543422019
C	-4.71609668843638	-5.85900687386865	0.96681171204783
C	-1.83586923456885	2.48682563146008	0.75706302071735
C	-3.42384260368299	-6.47728642909898	1.13617879963153
C	-1.23856897331439	3.68227641638550	0.30509046648424
C	0.13295202172925	3.83680294756591	0.28080677603152
C	0.95901194413290	2.79588306583865	0.72538244360423
C	0.39122028754231	1.61491575465740	1.22446124429198
C	-0.98518936375196	1.47031291893193	1.23156274698807
C	-3.36340580414247	-7.87988031212931	1.28268386114914
C	-2.16256113798843	-8.52694644408531	1.49528791102724
C	-0.99626976262687	-7.76515378135090	1.56378688913581
C	-1.01400546874579	-6.37711027248709	1.40057520043668
C	-2.21777651926601	-5.74400109106787	1.18567551082313
O	2.29885196098207	3.02429963332354	0.63110331839133
N	0.25208564080762	-8.41478032048158	1.87858381606079
O	1.25805775292496	-7.71428377327637	2.05001302806188
O	0.27265561458737	-9.64748825521153	1.98743542335406
C	3.19606988689713	1.97147876631237	1.07522767793760
C	4.56945730369695	2.32311813544539	0.64790657753771
N	5.46743701323649	2.95676938060574	1.45898390696916
N	6.59588113848158	3.09618636561383	0.81837044412785
N	6.42199312488546	2.58561304051071	-0.42397398645151
C	5.17993076817359	2.07386320784337	-0.55931850444656
C	7.57747621558065	2.35610264956990	-1.28358247516759
C	8.18372818213787	1.00201355602777	-0.88807087716055
O	9.26630255114662	0.92465272379887	-0.31229378243742
H	-6.15706476806239	3.14797056536955	0.56715850152501
H	-7.69829276968935	-5.62781388142925	0.89862023476277
F	-9.70919140545455	-1.17115120032177	-1.68923919416101
F	-12.37483398361742	-0.72687138628317	-1.85094634478670
F	-12.51406659348120	0.12910985439418	2.78504976114804
F	-9.84846836222871	-0.31162271915148	2.94727175190678
H	-8.70554833844772	3.27602591929116	0.30649677741221
H	-9.50365757412292	2.11211881048121	1.37514624808459
H	-9.48829673580506	1.83244640303894	-0.36623696459013
H	-10.48950715990165	-3.25692047494868	1.54882459637993
H	-10.14268374398693	-4.89319458533159	0.95903902190172
H	-10.39608129535651	-3.56928723982168	-0.18543764455899
H	-4.11885639987085	-3.83674634069014	1.14782526850695
H	-3.39933574005045	0.26782265283585	1.03915593964566
H	-3.82342708182920	3.25724265028286	0.44941236675983
H	-5.54970885217118	-6.54146636919811	0.82544088719868
H	-1.87374182325116	4.48943617433476	-0.05092478013425

H	0.58665964290677	4.75245856456493	-0.08624526326191
H	1.00556417308398	0.80894385705844	1.60823244926687
H	-1.40009316534733	0.54645901917580	1.62401890057242
H	-4.28416881959233	-8.45549232608928	1.24779012123158
H	-2.12800083315936	-9.60105541024562	1.63467367219465
H	-0.09411690215993	-5.80647028502643	1.45887875423438
H	-2.22378558123424	-4.66600018793568	1.06201333805469
H	2.90317811602340	1.02059304470262	0.61574238227868
H	3.13858135863728	1.88655434898262	2.16658882947784
H	4.84065564773997	1.59184375753627	-1.46367207558535
H	8.30443982766917	3.15340540455506	-1.12370751912371
H	7.24740264943828	2.34396023581624	-2.32504071823955
O	7.37346318733760	0.02574886219068	-1.18770765906697
Pt	7.39751151975226	-1.78454758205737	-0.20919425244610
N	7.45464267800355	-0.74061691775320	1.59026473182957
Cl	7.33639868742110	-2.91723490393281	-2.27911913676881
Cl	5.03327566626830	-1.60644741077787	-0.12253525943705
H	8.40856175649120	-0.50223987738347	1.85862381442339
H	7.03010947987009	-1.30460320709596	2.33216600344916
H	6.90897204633573	0.11801982877415	1.50036572254692
O	7.18944405847608	-3.59799648645961	0.70679873677238
C	7.88273787422757	-3.91379350401406	1.77882442229670
C	7.46565405795601	-5.23292912992914	2.37193322568889
H	7.01102481780865	-5.03058420654754	3.34804627442315
H	6.75191817966959	-5.76753761127398	1.74462142767707
H	8.35744670258139	-5.84400196912833	2.53672216568892
O	8.77461238237449	-3.22411559689356	2.27878893573574
N	9.46652965819758	-1.96020713534262	-0.25986216451894
H	9.86324952174817	-1.01875968923099	-0.32933879361741
H	9.75520162687026	-2.52179701032220	-1.05946304377031
H	9.76604451574267	-2.40948108175228	0.60825154223678
B	-2.19217113424427	-7.27998536987576	5.14809588788818
N	-3.01848942807525	-6.03258131983259	4.73908329623764
C	-4.40214096044344	-6.00305238585639	4.77405078269118
C	-5.13664030669248	-7.19682955353745	4.89332679253939
C	-4.49943459969382	-8.43127909240282	4.93084101429761
N	-3.11110487154689	-8.51183994934891	4.93447859539778
C	-2.75479524049990	-9.82952758587636	4.92175103636716
C	-3.94405328939117	-10.61368755134580	4.90743413852970
C	-5.02880620404965	-9.77051246772238	4.92775945519786
C	-4.83630445182130	-4.65212010276426	4.58210942119162
C	-3.68933093224803	-3.90376864695802	4.40477829234939
C	-2.56791562645861	-4.75956995849791	4.50339447651852
F	-1.83653007453935	-7.18598663830103	6.51293472420227
F	-1.02136663007881	-7.38310293336836	4.38801052688176
C	-6.61681382495375	-7.11628292739459	4.94310734268527
C	-7.27491766305214	-6.84235280930253	6.13559222191422
C	-8.65289536710458	-6.70461268640022	6.19800416619000
C	-9.40299142942337	-6.83408275082558	5.03753604278815
C	-8.77388444249745	-7.11455963496856	3.83282490539956
C	-7.39651537415004	-7.26109565207063	3.80351179541227
F	-10.72834876498505	-6.69306999281358	5.08039506159992
C	-6.45519877484201	-10.20035022048610	4.91919586096203
C	-6.22140978463693	-4.10120388492670	4.53494185456265
C	-1.18834562874314	-4.43312989710285	4.34731344741839
C	-1.40082884064536	-10.26560466015761	4.91874081939923
C	-1.04035322343928	-11.57670187469129	4.85210580406121
C	-0.75348321514056	-3.18824974090325	4.01626059735595
C	0.30881373489853	-12.07864319672261	4.79083850144904
C	0.62303122333592	-2.81713254090168	3.80428133470115
C	0.51260979468593	-13.47537959623021	4.78099708402313
C	1.77861309213317	-14.01823743046948	4.71098575412746
C	2.89350542479394	-13.17262303578491	4.64108009363245
C	2.72282024520842	-11.78079789902390	4.64636762569599
C	1.44653149863580	-11.25112827190431	4.72043965711854
C	0.93203223788697	-1.44475900574053	3.68779422190287
C	2.23202706307554	-1.01336261233808	3.52850482671072
C	3.25143761906889	-1.96503753897859	3.46392513380300
C	2.98131445649934	-3.33604582470883	3.54245829085800
C	1.67830930911880	-3.75393421351073	3.70632751205665
O	4.10131918276211	-13.79559594938574	4.57303271374685
N	4.60942571265198	-1.51776180839433	3.31963966825442
O	5.52023646657760	-2.36301816295961	3.31687819369612
O	4.83013527098695	-0.30655286570722	3.19658594455888
C	5.28213918114881	-12.96558405942767	4.41858887361871
C	6.45201850555225	-13.86891810670730	4.33236371044065
N	6.71623539811143	-14.62585143932242	3.22638192907618

N	7.79500329959201	-15.32850732377056	3.44128719610467
N	8.22349595008748	-15.04280340780837	4.68725258583092
C	7.42291676934553	-14.12451876071276	5.27135220154566
C	9.50427053146337	-15.53448931860820	5.15233915250332
C	10.69686365771644	-14.68596237682869	4.71496013221583
O	11.83187563971573	-15.07668384245909	4.98195173394040
H	-3.98358850330699	-11.69411097733918	4.88700720246993
H	-3.65751041709872	-2.84185325942539	4.20892320300899
F	-6.56704692767609	-6.68830528329555	7.26290868758953
F	-9.26049121608885	-6.43943227132247	7.35842758324113
F	-9.49767811109666	-7.23727276816768	2.71535649819051
F	-6.81088631882700	-7.54189617922070	2.63212759213194
H	-6.51083401899810	-11.28462566142584	5.04454666496125
H	-6.94531952221600	-9.94792258828702	3.97202753041842
H	-7.03188526405964	-9.72708007914142	5.72036623961812
H	-6.81496943236788	-4.54019155330361	3.72468247635954
H	-6.17472148021125	-3.02109466568835	4.37313620144865
H	-6.76621527509089	-4.27866301726420	5.46863121931487
H	-0.47219448278357	-5.23624506584459	4.48266703330934
H	-0.63655701587672	-9.49762181164679	4.95293567690607
H	-1.81843393416670	-12.33859116579431	4.83212533734573
H	-1.47528214190802	-2.38001769048264	3.91303013957170
H	-0.34990179736372	-14.13514640183328	4.83020679701268
H	1.92836910626150	-15.09360132042431	4.70389238623064
H	3.57129022784345	-11.10932138639008	4.58986599804838
H	1.34000756170513	-10.17066909880503	4.71812755409593
H	0.12908523873599	-0.71494673947052	3.74513309354711
H	2.46331678275108	0.04345600940729	3.46603228921767
H	3.78700270621244	-4.05684585849978	3.46647126525990
H	1.47364201272125	-4.81901083182458	3.75003281896410
H	5.38514076561898	-12.29886947730615	5.28189658102138
H	5.18207356033885	-12.36775849154474	3.50430947147464
H	7.59836368406895	-13.74313632208173	6.26676794000265
H	9.65832280528631	-16.54973870878013	4.77528043128240
H	9.49830572039015	-15.57082645523881	6.24591546777699
O	10.36232110507903	-13.59713987131977	4.09173361034907
Pt	11.75137396595155	-12.31515049432089	3.28526458011564
N	12.78021731554402	-13.89525126582682	2.40240759872044
Cl	10.56932251582005	-10.53444212203852	4.28737342271321
Cl	10.39572446198320	-12.27602330975911	1.34575744311754
H	13.48726524833585	-14.27765455952041	3.02832226336048
H	13.23842063299473	-13.57293440779636	1.55097096314895
H	12.12292279298433	-14.63630904398934	2.15947222237996
O	12.94408918248025	-10.92626120247803	2.37825731268902
C	14.25494524362390	-11.03079713082884	2.36199975717327
C	14.91221410160185	-9.93637554407148	1.56493985767016
H	15.26480561156563	-10.37487292254789	0.62463320910079
H	14.22965884296979	-9.11591190386574	1.34168939174669
H	15.78329305017383	-9.57075573704269	2.11448081867876
O	14.90618860433816	-11.92301274986587	2.91108769705928
N	12.95402345810279	-12.37466677781737	4.97863211297915
H	12.84023551893612	-13.28118101149843	5.43665615628273
H	12.69799448211518	-11.62539455640483	5.61997515849659
H	13.92536340185815	-12.26230861299578	4.67750545675844

5.9. MTT assay

Human breast adenocarcinoma Sk-Br-3 cells were seeded in 96-well plates (10^4 cells per well) in complete DMEM medium. The following day, the medium in some wells was replaced with 100 µl of fresh medium containing **BODIPY-NPs** in the concentration range of 60-1.87 µM (including control points and negative control). The cells were incubated with nanoparticles for 1 h, after which they were irradiated at a wavelength of 650 nm (90 mW/cm^2) for 13 min; non-irradiated cells served as a control. Cell viability was assessed after 72 h using the MTT assay. For this, an MTT solution (0.5 mg/ml) was added to each well. After 2 h, the medium was removed and 100 µl of DMSO (99%) was added. Optical density was recorded at 565 nm on an Infinite M Nano reader (Tecan, Switzerland).

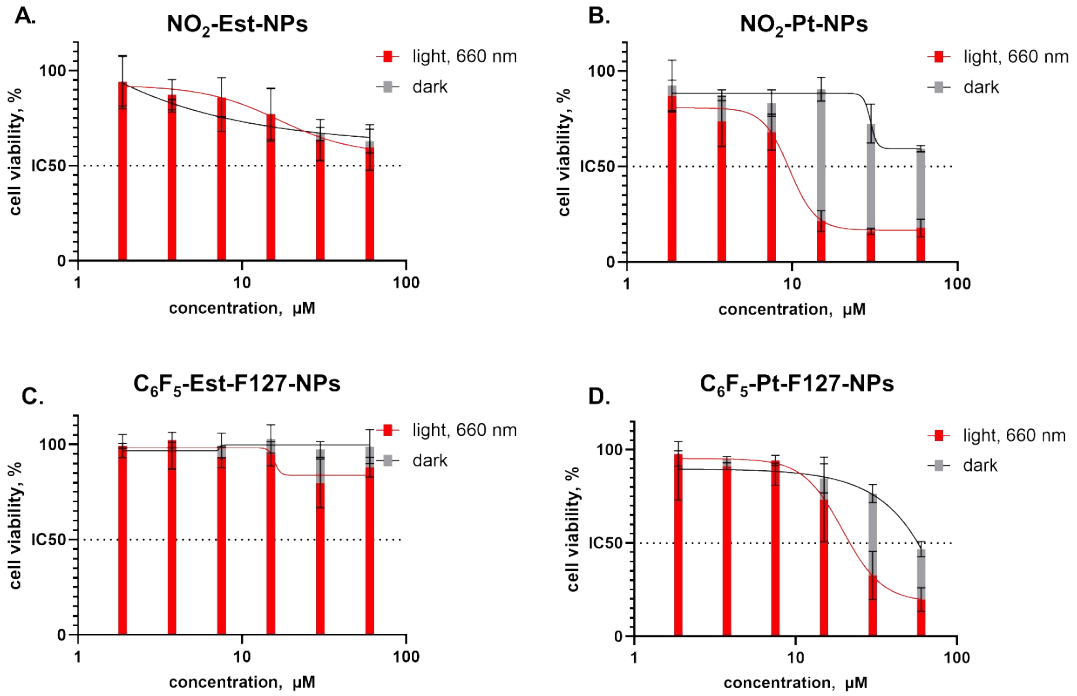

Figure S39. Cell viability of Sk-Br-3 cells incubated with **BODIPY-NPs** at various concentrations in the dark and after LED light irradiation (650 nm, 13 min, 90 mW/cm^2). A. **NO_2-Est-NPs.** B. **NO_2-Pt-NPs**. C. **C_6F_5-F127-NPs**. D. **C_6F_5-Pt-F127-NPs.**

References

(1) Tietze, L. F.; Eicher, T. *Reaktionen Und Synthesen Im Organisch-chemischen Praktikum Und Forschungslaboratorium*; Wiley, 1991. https://doi.org/10.1002/3527601716.

(2) Spector, D. V.; Bykusov, V.; Zharova, A.; Kuzmichev, I.; Isaeva, Y. A.; Khaydukov, E. V.; Trifanova, E.; Stepanov, M.; Erofeev, A. S.; Gorelkin, P.; Kuanaeva, R.; Nikitina, V. N.; Dubenskii, A.; Maksimova, Y.; Skvortsov, D. A.; Ipatova, D.; Rodin, I. A.; Vokuev, M. F.; Martynov, A. G.; Bunin, D.; Pokrovsky, V. S.; Babayeva, G.; Uskova, T.; Abakumov, M. A.; Beloglazkina, E. K.; Akasov, R. A.; Krasnovskaya, O. O. Nanoformulation of the Photoactive Cisplatin Prodrug for Combined Photothermal Therapy and Bioimaging. *ACS Appl Nano Mater* **2024**. https://doi.org/10.1021/acsanm.4c04680.

(3) Atilgan, A.; Beldjoudi, Y.; Yu, J.; Kirlikovali, K. O.; Weber, J. A.; Liu, J.; Jung, D.; Deria, P.; Islamoglu, T.; Stoddart, J. F.; Farha, O. K.; Hupp, J. T. BODIPY-Based Polymers of Intrinsic Microporosity for the Photocatalytic Detoxification of a Chemical Threat. *ACS Appl Mater Interfaces* **2022**, *14* (10), 12596–12605. https://doi.org/10.1021/acsami.1c21750.

(4) Aydın Tekdaş, D.; Viswanathan, G.; Zehra Topal, S.; Looi, C. Y.; Wong, W. F.; Min Yi Tan, G.; Zorlu, Y.; Gürek, A. G.; Lee, H. B.; Dumoulin, F. Antimicrobial Activity of a Quaternized BODIPY against Staphylococcus Strains. *Org Biomol Chem* **2016**, *14* (9), 2665–2670. https://doi.org/10.1039/C5OB02477C.

(5) Zaibudeen, A. W. Recent Advances in Different Nanoprecipitation Methods for Efficient Drug Loading and Controlled Release. *Journal of Nanotechnology and Nanomaterials* **2025**, *6* (1), 12–25. https://doi.org/10.33696/Nanotechnol.6.059.

(6) Yaminsky, I.; Akhmetova, A.; Meshkov, G. Femtoscan Online Software and Visualization of Nano-Objecs in High-Resolution Microscopy. *Nanoindustry Russia* **2018**, No. 6, 414–416. https://doi.org/10.22184/1993-8578.2018.11.6.414.416.

(7) Wang, Z.; Gai, S.; Wang, C.; Yang, G.; Zhong, C.; Dai, Y.; He, F.; Yang, D.; Yang, P. Self-Assembled Zinc Phthalocyanine Nanoparticles as Excellent

Photothermal/Photodynamic Synergistic Agent for Antitumor Treatment. *Chemical Engineering Journal* **2019**, *361*, 117–128. https://doi.org/10.1016/j.cej.2018.12.007.
(8) Li, X.; Lee, D.; Huang, J.; Yoon, J. Phthalocyanine-Assembled Nanodots as Photosensitizers for Highly Efficient Type I Photoreactions in Photodynamic Therapy. *Angewandte Chemie International Edition* **2018**, *57* (31), 9885–9890. https://doi.org/10.1002/anie.201806551.
(9) Daghastanli, N. A.; Itri, R.; Baptista, M. S. Singlet Oxygen Reacts with 2′,7′-Dichlorodihydrofluorescein and Contributes to the Formation of 2′,7′-Dichlorofluorescein. *Photochem Photobiol* **2008**, *84* (5), 1238–1243. https://doi.org/10.1111/j.1751-1097.2008.00345.x.
(10) Xi, D.; Xiao, M.; Cao, J.; Zhao, L.; Xu, N.; Long, S.; Fan, J.; Shao, K.; Sun, W.; Yan, X.; Peng, X. NIR Light-Driving Barrier-Free Group Rotation in Nanoparticles with an 88.3% Photothermal Conversion Efficiency for Photothermal Therapy. *Advanced Materials* **2020**, *32* (11), 1907855. https://doi.org/10.1002/adma.201907855.
(11) Neese, F. Software Update: The <scp>ORCA</Scp> Program System—Version 5.0. *WIREs Computational Molecular Science* **2022**, *12* (5). https://doi.org/10.1002/wcms.1606.
(12) Neese, F.; Wennmohs, F.; Becker, U.; Riplinger, C. The ORCA Quantum Chemistry Program Package. *J Chem Phys* **2020**, *152* (22). https://doi.org/10.1063/5.0004608.
(13) Lu, T.; Chen, F. Multiwfn: A Multifunctional Wavefunction Analyzer. *J Comput Chem* **2012**, *33* (5), 580–592. https://doi.org/10.1002/jcc.22885.
(14) Grimme, S.; Hansen, A.; Ehlert, S.; Mewes, J.-M. R2SCAN-3c: A “Swiss Army Knife” Composite Electronic-Structure Method. *J Chem Phys* **2021**, *154* (6). https://doi.org/10.1063/5.0040021.
(15) Marenich, A. V.; Cramer, C. J.; Truhlar, D. G. Universal Solvation Model Based on Solute Electron Density and on a Continuum Model of the Solvent Defined by the Bulk Dielectric Constant and Atomic Surface Tensions. *J Phys Chem B* **2009**, *113* (18), 6378–6396. https://doi.org/10.1021/jp810292n.
(16) Weigend, F.; Ahlrichs, R. Balanced Basis Sets of Split Valence, Triple Zeta Valence and Quadruple Zeta Valence Quality for H to Rn: Design and Assessment of Accuracy. *Physical Chemistry Chemical Physics* **2005**, *7* (18), 3297. https://doi.org/10.1039/b508541a.
(17) Pantazis, D. A.; Chen, X.-Y.; Landis, C. R.; Neese, F. All-Electron Scalar Relativistic Basis Sets for Third-Row Transition Metal Atoms. *J Chem Theory Comput* **2008**, *4* (6), 908–919. https://doi.org/10.1021/ct800047t.
(18) Bannwarth, C.; Ehlert, S.; Grimme, S. GFN2-XTB—An Accurate and Broadly Parametrized Self-Consistent Tight-Binding Quantum Chemical Method with Multipole Electrostatics and Density-Dependent Dispersion Contributions. *J Chem Theory Comput* **2019**, *15* (3), 1652–1671. https://doi.org/10.1021/acs.jctc.8b01176.